PAHs in space: investigating their spectra

F. I. Giasemis
Astrophysics, Department of Physics
University of Oxford

June/July 2018

Abstract

The purpose of this project is to investigate Polycyclic Aromatic Hydrocarbons (PAHs) found in space. We need to understand PAHs because on the one hand they allow us to probe the interstellar medium and on the other hand they can be used to trace star formation in galaxies. Since PAHs are highly complicated atoms, computational methods such as Density Functional Theory (DFT) will be used to calculate their electronic structure. Then, for PAHs that are found in space such as coronene and circumcoronene, their spectra will be predicted using the computational models for their electronic structure. By comparing our results with observations, we can draw serious conclusions about our computational models and the assumptions behind them. The aim of the project is to use these models to understand the properties of PAH molecules in space.

Spectra were calculated for various PAH molecules, including coronene, circumcoronene and pentacene, as well as some interesting cases of PANHs. Finally, data from the UKIRT around the 3.3 μm feature were used to hypothesize the origin of the 3.3 and 3.4 PAH emission bands from NGC 7027.

1 Introduction

Polycyclic aromatic hydrocarbons (PAHs) are thought to be the most abundant class of organic compounds in the Universe. The infrared spectra of many galactic and extragalactic objects are dominated by emission features at 3.3, 6.2, 7.7, 8.6 and 11.2 microns. The origin of these features remained a mystery and the bands became known as the unidentified infrared (UIR) bands. Since the mid-80s, the UIR bands are generally attributed to PAH molecules. Their excitation generally proceeds by absorption of ultraviolet photons through electronic transitions, followed by internal energy redistribution, leaving PAHs in highly excited vibrational states. PAHs then cool by fluorescence, emitting infrared photons at the frequencies corresponding to these vibrational modes. The ubiquity of PAHs and their prominence in the mid-infrared spectra of star-forming regions make them potentially powerful tools for studying star formation throughout the Universe. Star formation is a fundamental property of galaxy formation and evolution. Understanding the exact star formation rate, and how it evolves with time and galaxy mass is at the heart of contemporary astronomical research. PAHs may even have links to the origin of life (PAH world hypothesis). Therefore, understanding how PAHs behave is really important.

2 First calculations (DFT)

The Gaussian (09) software was used along with Gaussview 5. First, calculations were done on benzene and pyrene. A Dunning basis set and the B3LYP level of theory were used. Results are shown in Fig. 4 and 5 in the Appendix. The spectrum of coronene is show in Fig. 6. In this case, the minimal basis set STO-3G was used.

3 Larger PAH Molecules (DFT/MM)

For larger molecules, we had to change the script from max output (`#p`) to terse or normal (`#t` and `#n`) to reduce the time of computation. Also, the maximum number of cycle was reduced to between 10 and 20.

3.1 $C_{44}H_{18}$

We started by stacking two coronenes side by side to produce a $C_{44}H_{18}$ neutral molecule.

3.2 $C_{36}H_{16}$

The next molecule was $C_{36}H_{16}$ with uid 154 in the PAH IR Spectral Database [1] [1] [2] [3]. We built it in Gaussview 5 and the result of the gaussian calculation is shown in Fig. 7. The result seems to agree with the results obtained from the database.

3.3 $C_{42}H_{18}$

The next molecule was $C_{42}H_{18}$ (uid 105) or hexa-peri-hexabenzocoronene. The gaussian calculation was crashing so we had to use `opt(...., restart)` to make it converge. The result is in Fig. 8.

3.4 $C_{54}H_{18}$

The next molecule of particular interest is circumcoronene or $C_{54}H_{18}$ with uid 37.

---

[1] `http://www.astrochem.org/pahdb/`

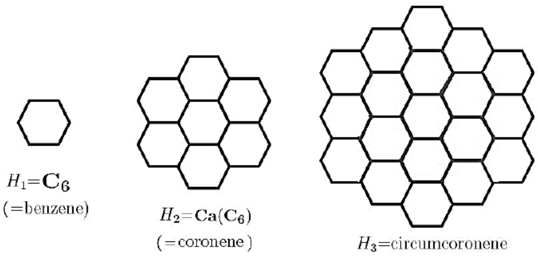

The DFT optimization calculations all failed to converge. Then, we use a simpler model, namely Molecular Mechanics (MM) that treats atoms as hard spheres and bonds as springs and does not calculate electronic orbitals etc. MM on its own can give results for the frequencies but not their relative intensitites because the IR intensitites depend on dipole moments and hence on charges. Charge Equilibration (QEq) is an approach for predicting charge distributions in molecules for use in MM or Molecular Dynamics (MD) that was developed by Rappe and Goddard in 1991. With QEq then it is possible to obtain the relative intensities and hence the spectrum of the molecule. From the Gaussview 5 interface, using the `Opt+Freq` option with `QEq=all atoms`, the gaussian calculation is shown in Fig. 9. We have to note that by comparing the MM method with DFT for coronene for example we see some discrepancies.

3.5 $C_{78}H_{22}$

The MM method for $C_{78}H_{22}$ (uid 120) also failed to converge, but then using the command `scf=qc` in the Route section we obtained the spectrum (Fig. 10).

3.6 $C_{66}H_{20}$

The $C_{66}H_{20}$ (uid 115) spectrum obtained using the MM method is shown in Fig. 11.

3.7 $C_{96}H_{24}$

The calculation for circumcircumcoronene or $C_{96}H_{24}$ (uid 108) resulted in the spectrum in Fig. 12.

Remark

The MM method returns almost the same spectrum for both neutral atoms and their cationic/anionic counterparts. We came to this conclusion after looking at several molecules like pentacene and coronene for which we know the 3 micron IR feature almost disappears for ionised states. This may be due to the simplicity of the model. More specifically, that the MM model does not calculate electron clouds etc., so the change in charge state does not make a difference in the result.

4 PANHs

Interesting PAH variants are polycyclic aromatic nitrogen heterocycles (PANHs). One or more carbon atoms are substituted with a Nitrogen atom. When this atom is on the circumference of the PAH, the molecule is called an *Exoskeletal* PANH, while if the Nitrogen is further in, it is called and *Endoskeletal* PANH. For some specific molecules we will use Fig. 2 of Hudgins et al. (2005) [4] to specify the position of the substituted Nitrogen.

4.1 Pyridine

First, we looked at pyridine with chemical formula C_5H_5N. It is structurally related to benzene with one =CH– group replaced by a nitrogen atom. The spectrum shows significant difference from the spectrum of the benzene molecule, both calculated with the MM method.

4.2 Circumcoronene

The spectrum for the exoskeletal PANH $C_{53}H_{18}N^+$ (uid 238) is calculated using MM/QEq. The result is shown in Fig. 13. Fig. 14 shows a comparison of the spectra between a circumcoronene and its variant.

5 Semi-Empirical Methods

DFT/B3LYP methods seem to reach the physical limit or the ARC [2] facility for $C > 50$. On the other hand, MM is a much more computationally cheap but also crude method. In between the two are the so-called Semi-Empirical methods.

5.1 $C_{54}H_{18}$

The calculation of the circumcoronene specrtrum with PM3MM is shown in Fig. 15.

5.2 $C_{22}H_{14}$

As a test for the quality of the results obtained from the PM3MM method, we calculated the spectra of neutral and cationic pentacene with chemical formula $C_{22}H_{14}$ as well as dehydrogenated cationic pentacene with formula $C_{22}H_{13}$. The results are shown in Fig. 16, 17 and 18 respectively. It is clear that the 3 μm feature is almost absent from the spectrum. This is in agreement with the literature results. As an example, we have Fig. 19 from the PAH IR spectral database.

5.3 $C_{66}H_{20}$

The spectrum for $C_{66}H_{20}$ with uid 115 is shown in Fig. 20.

5.4 $C_{96}H_{24}$

The spectrum for $C_{96}H_{24}$ with uid 108 is shown in Fig. 21. Also, the spectrum for dehydrogenated cationic circumcircumcoronene $C_{96}H_{23}^+$ was obtained (Fig. 22).

---

[2] `http://www.arc.ox.ac.uk/content/home`

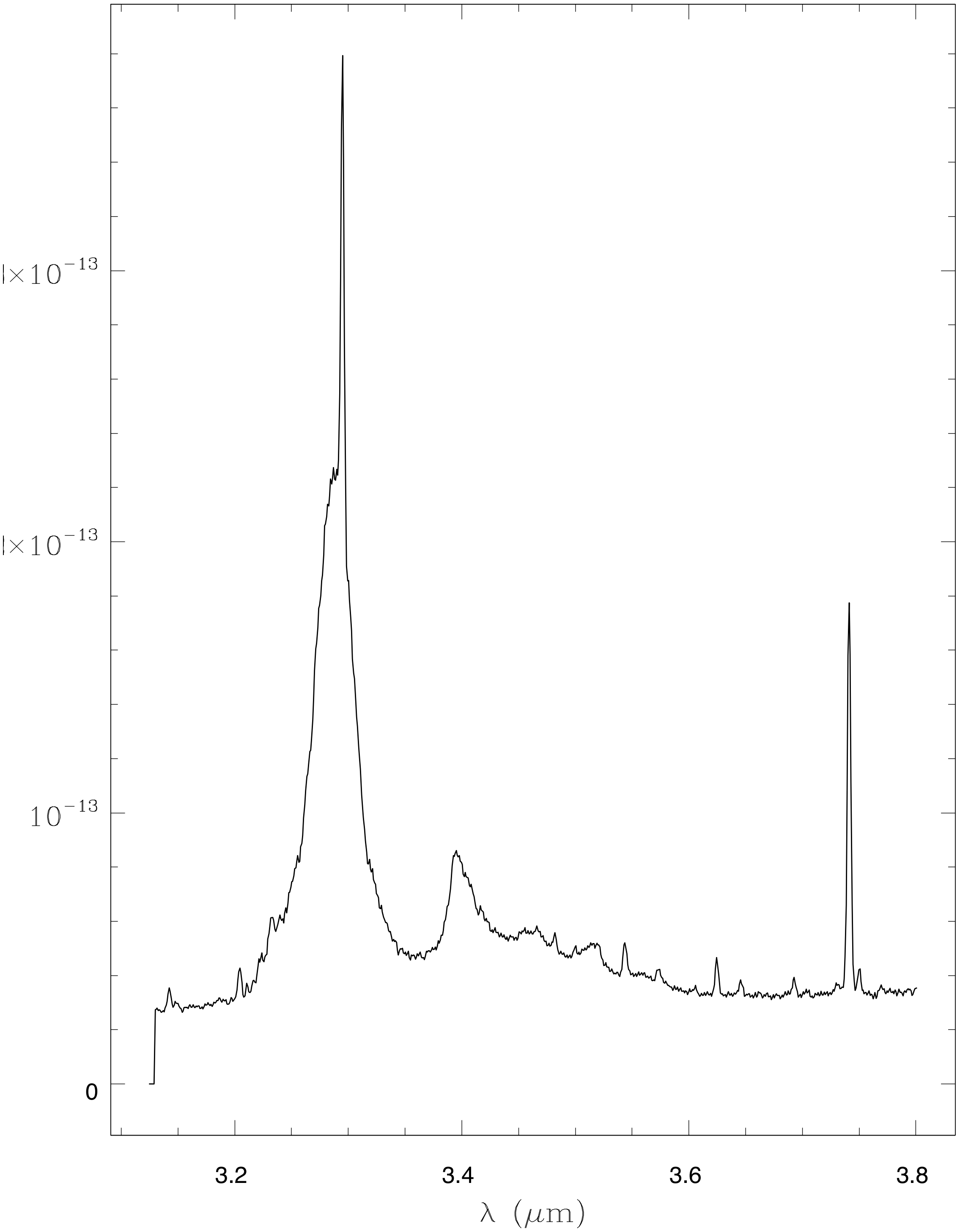

Figure 1: The 3 micron feature of the planetary nebula NGC 7027 (UKIRT).

5.5 $C_{53}H_{18}N^{+}$

The spectrum of $C_{53}H_{18}N^{+}$ (position 1 in [4]) this time was calculated using the semi-empirical method PM3MM and the result is shown in Fig. 23. Comparing Fig. 14, 15 and 23, the results seem to agree very well. Next, the substituted nitrogen was placed in position 5 [4]. The result is shown in Fig. 24.

5.6 $C_{112}H_{26}$

The next large molecule, $C_{112}H_{26}$ with uid 165, is shown in Fig. 25. Some of the molecules we calculated can be found in [5].

6 Circumcoronene PANHs

We have already calculated singly-substituted circumcoronene PANHs at positions 1 and 5.

6.1 Singly substituted PANHs

The calculations for nitrogen at positions 1', 2, 3 and 4 give the results shown in Fig. 26-29 respectively.

6.2 Multiply substituted PANHs

Some examples of the calculations are shown in Fig. 30-31. For the positions of the nitrogens again we use Fig. 2 of [4].

7 UKIRT 3 μm feature of NGC 7027

The 3 micron feature of the planetary nebula NGC 7027 obtained with the United Kingdom Infrared Telescope (UKIRT) in 1995 is shown in Fig. 1. PAHs are the of 3.3 and 3.4 micron emission bands [6]. On top of that we observe hydrogen recombination lines at 3.74 μm as well as at 3.3 μm (line Pfβ), overlapping the PAH feature [7].

7.1 The 3.3 and 3.4 micron PAH features

We note that the ratio of intensities of the the 3.3 and 3.4 μm features is

$$\lambda \approx 11/4 \approx 2.8.$$

We then searched for PANHs that have a feature at 3.4 and 3.3 microns. An interesting candidate is the circumcoronene PANH $C_{52}H_{18}N_2^{++}$. Another molecule that produces a similar spectrum is the coronene counterpart of the previous one, i.e. $C_{22}H_{12}N_2^{++}$ as well as circumcircumcoronene with the 2 nitrogens substituted in approximately the same locations. A first possible scenario for the origin of the PAH features is the following: a population of doubly substituted cationic (+2) exoskeletal highly symmetric (coronene-like) PANHs. Also, from [6], another possibility is a molecule produced by attaching a methyl group to a PAH, e.g. methyl-coronene. Some interesting cases are shown in Fig. 32-34. In Fig. 35 a comparison between the spectrum of $C_{52}H_{18}N_2^{++}$ and the experimental data is shown, focusing in the 3 micron area. The same was done for $C_{94}H_{24}N_2^{++}$ as well as $C_{22}H_{12}N_2^{++}$.

7.2 Methyl groups

We also looked at methylcoronene. In Fig. 37 we used DFT to calculate the spectra. In the next two figures we focus on the interesting areas of the spectrum. In Fig. 40 a comparison of $C_{23}H_{15}N_2^{++}$, the $C_{22}H_{12}N_2^{++}$ above with a methyl group attached, with NGC 7027.

8 MIR Spectra

We used data for the mid infrared (MIR) spectra of NGC 7027 and NGC 23 from Spitzer IRS. Since, the data from UKIRT cover a narrow range of wavelengths, we can look how the candidates (gaussian models) matching the 3 micron feature compare to the mid-IR spectra of the same object, i.e. NGC 7027.

8.1 NGC 7027

The spectrum for NGC 7027 is shown in Fig. 2.

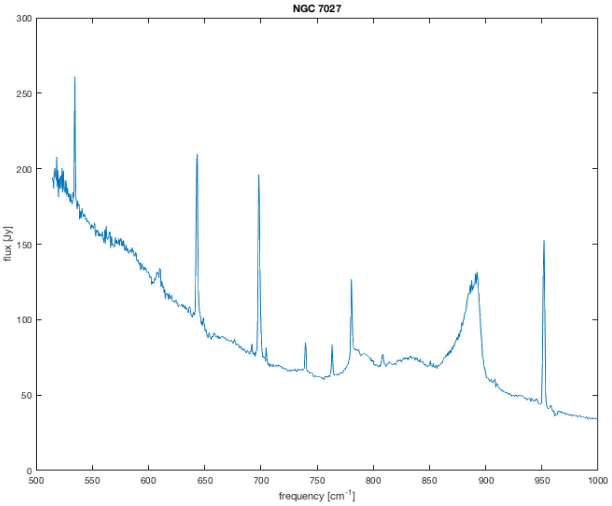

Figure 2: The MIR spectrum of NGC 7027 (Spitzer IRS).

We focused on the feature between 850 and 900 cm^{-1}. Looking at Fig. 38 for 1-methylcoronene, we see that indeed between 850 and 950 cm^{-1} we get two large spikes. Since, this is a DFT calculation, some scaling factors are involved which we have not taken into account. Also, in Fig. for $C_{52}H_{18}N_2^{++}$ we observe a spike at the same area. Furthermore, going back to Fig. 5 for pyrene and coronene (DFT), we observe lines at around 900 cm^{-1}. Therefore, the broadness of the feature can be explained by a variety of PAHs emitting at slightly different frequencies around $\sim 850 - 900$ cm^{-1}. A comparison of the NGC7027 spectrum with the DFT methylocoronene model is shown in Fig. 41

8.2 NGC 23

The spectrum for NGC 23 is shown in Fig. 3.

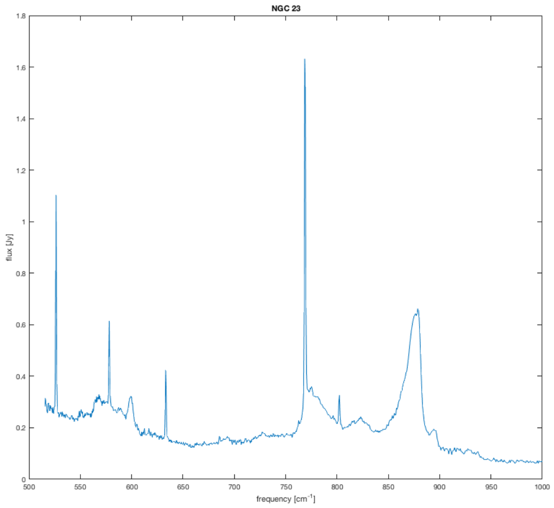

Figure 3: The MIR spectrum of NGC 23 (Spitzer IRS).

We focused on the features 750−800 cm^{-1} and 850−900 cm^{-1}. Again, the pyrene spectrum (DFT), Fig. 5, seems to match the spectrum at this area particularly well.

8.3 Identifying a PAH/PANH population

In Fig. 35-46 are examples of comparisons between intersting candidates and real spectra.

References

[1] C.W. Bauschlicher, Jr., A. Ricca, C. Boersma, L.J. Allamandola, "The NASA Ames PAH IR Spectroscopic Database: Computational Version 3.00 with Updated Content and the Introduction of Multiple Scaling Factors", ApJ Supplement Series, 234, 32, Feb 2018.

[2] C. Boersma, C.W. Bauschlicher, Jr., A. Ricca, A.L. Mattioda, J. Cami, E. Peeters, F. Snchez de Armas, G. Puerta Saborido, D.M. Hudgins, and L.J. Allamandola, "The NASA Ames PAH IR Spectroscopic Database Version 2.00: Updated Content, Website And On/Offline Tools", ApJ Supplement Series, 211, 8, Mar 2014.

[3] A. L. Mattioda, D. M. Hudgins, C. Boersma, A. Ricca, E. Peeters, J. Cami, F. Sanchez de Armas, G. Puerta Saborido, C. W. Bauschlicher, Jr ., and L. J. Allamandola, "The NASA Ames PAH IR Spectroscopic Database Version 2.00: Updated Content, Website And On/Offline Tools", ApJ Supplement Series, XXX, 201X (in preparation)

[4] D. M. Hudgins, C. W. Bauschlicher, Jr. and L. J. Allamandola, "Variations in the Peak Position of the 6.2 m Interstellar Emission Feature: A Tracer of N in the Interstellar Polycyclic Aromatic Hydrocarbon Population", ApJ, 632, 316-332, Oct 2005.

[5] C. W. Bauschlicher, Jr., E. Peeters, and L. J. Allamandola, "The Infrared Spectra of Very Large, Compact, Highly Symmetric, Polycyclic Aromatic Hydrocarbons (PAHs)", ApJ, 678, 316-327, May 2008.

[6] C. Joblin, A. G. G. M. Tielens, L. J. Allamandola, A. Leger, L. d'Hendecourt, T. R. Geballe, P. Boissel, "PAHs as the carriers of the 3.3 and 3.4 um emission bands", Planet. Space Sci., Vol. 43, Nos. 10/11, 1189-1194, Jan 1995.

[7] B. van Diedenhoven, E. Peeters, C. Van Kerckhoven, S. Hony, D. M. Hudgins, L. J. Allamandola, and A. G. G. M. Tielens, "The Profiles of the 3-12 micron Polycyclic Aromatic Hydrocarbon Features", ApJ, 611, 928-939, Aug 2004.

9 Appendix: Figures

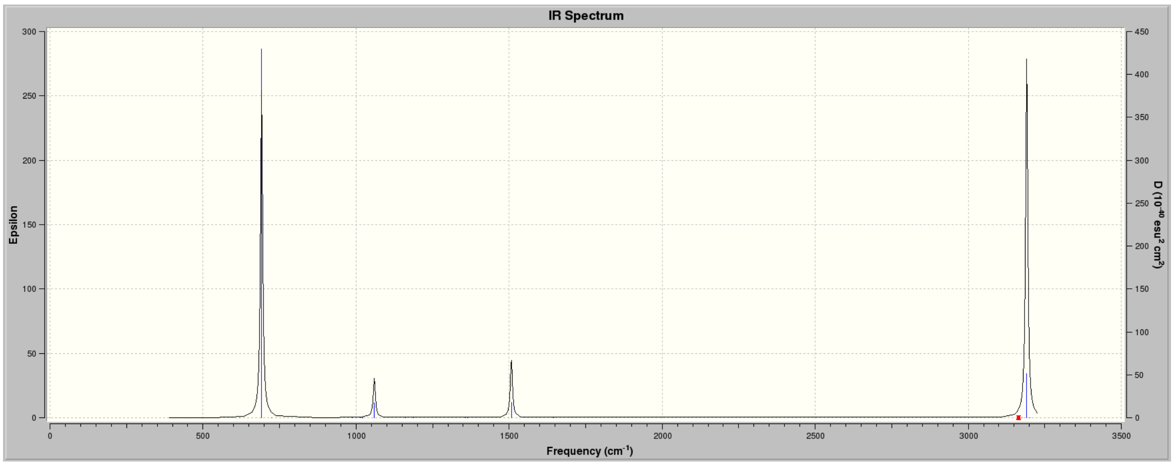

Figure 4: Benzene spectrum.

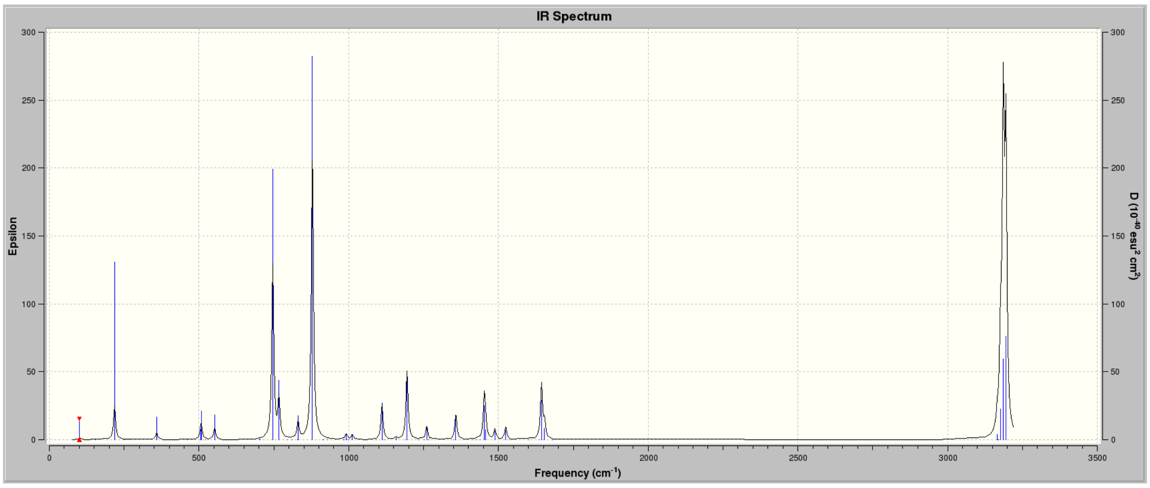

Figure 5: Pyrene spectrum.

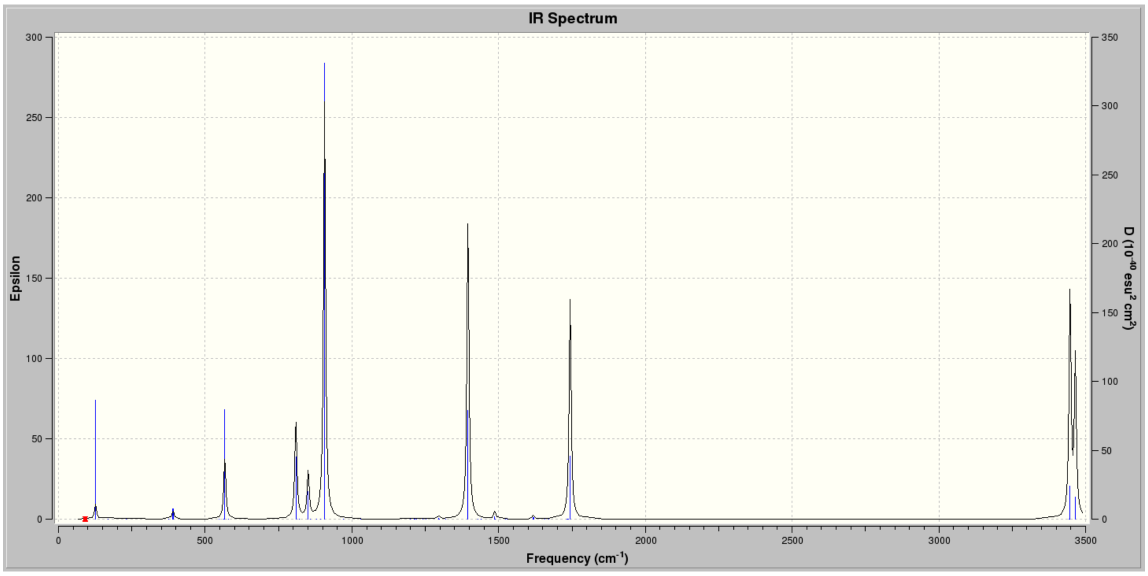

Figure 6: Coronene spectrum.

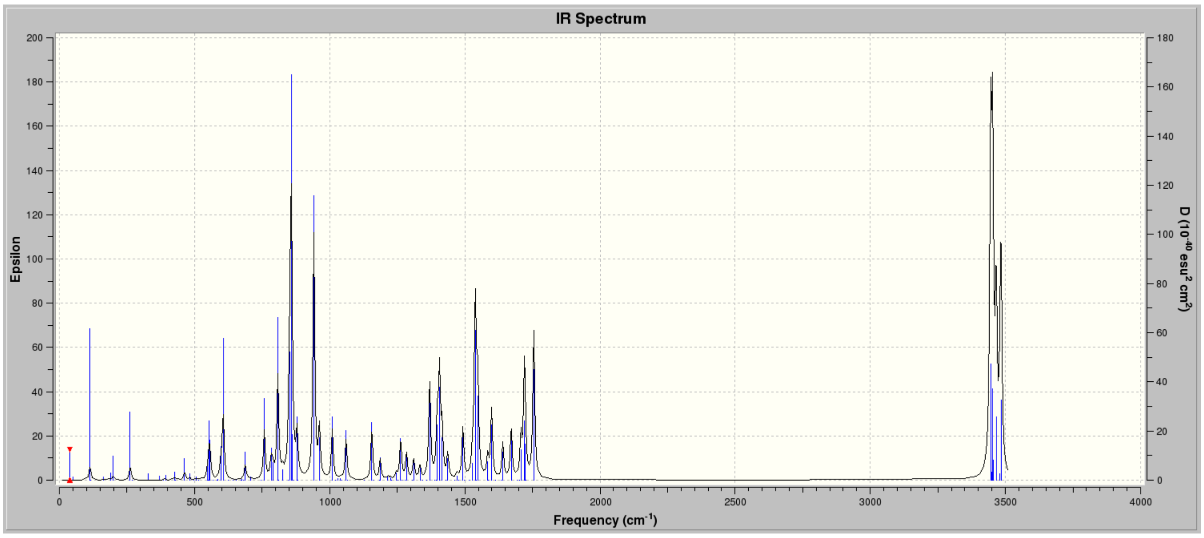

Figure 7: $C_{36}H_{16}$ spectrum.

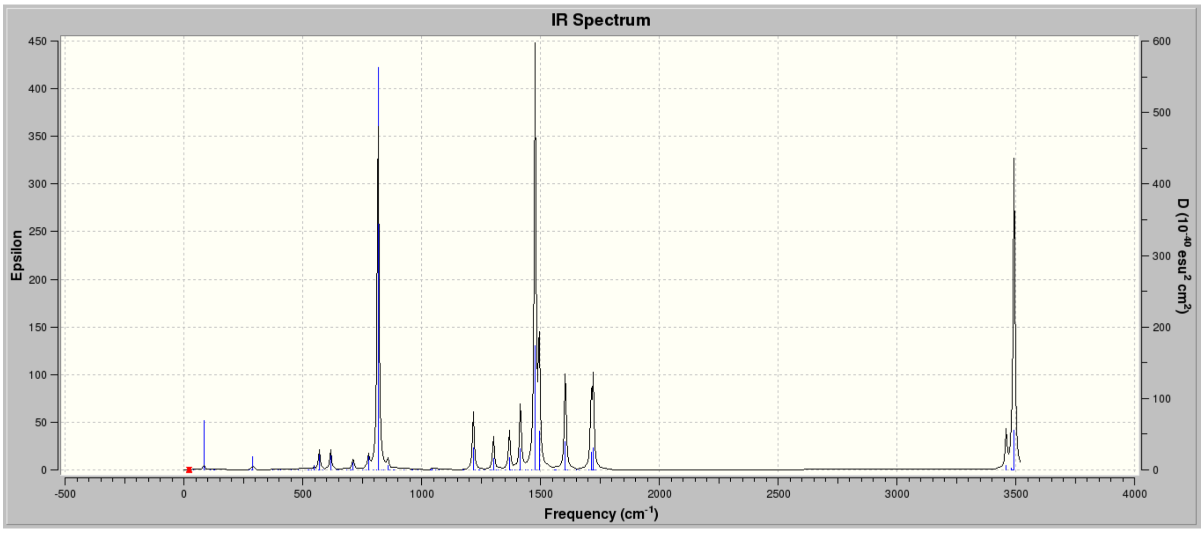

Figure 8: Hexabenzocoronene spectrum.

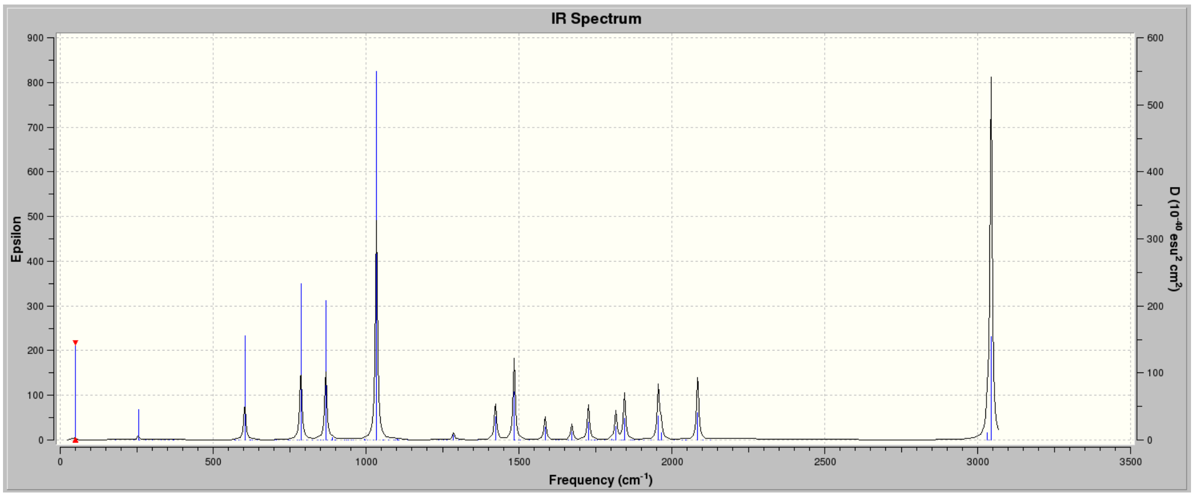

Figure 9: Circumcoronene spectrum, using the MM method.

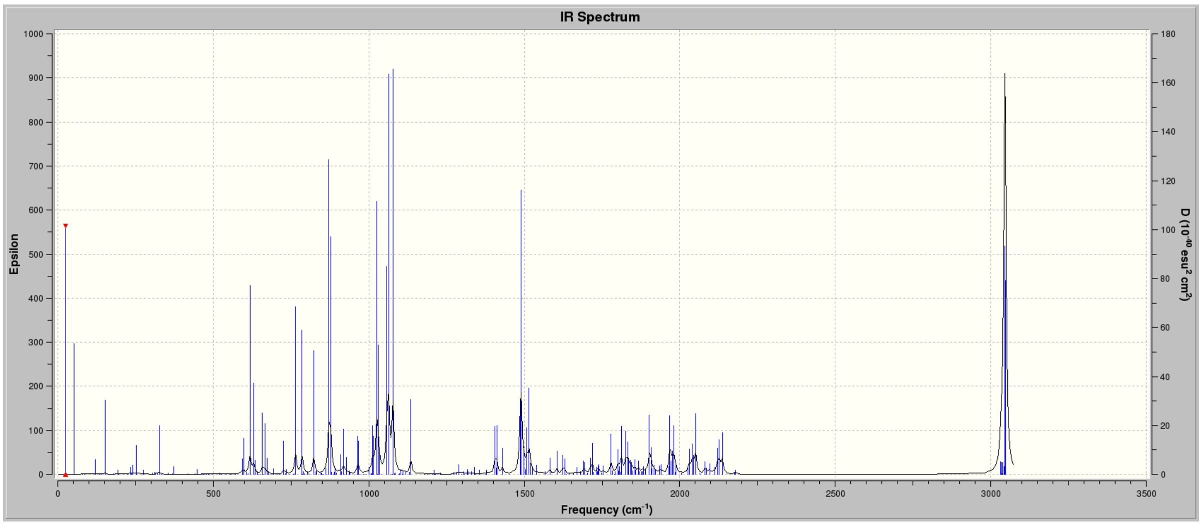

Figure 10: $C_{78}H_{22}$ spectrum, using the MM method.

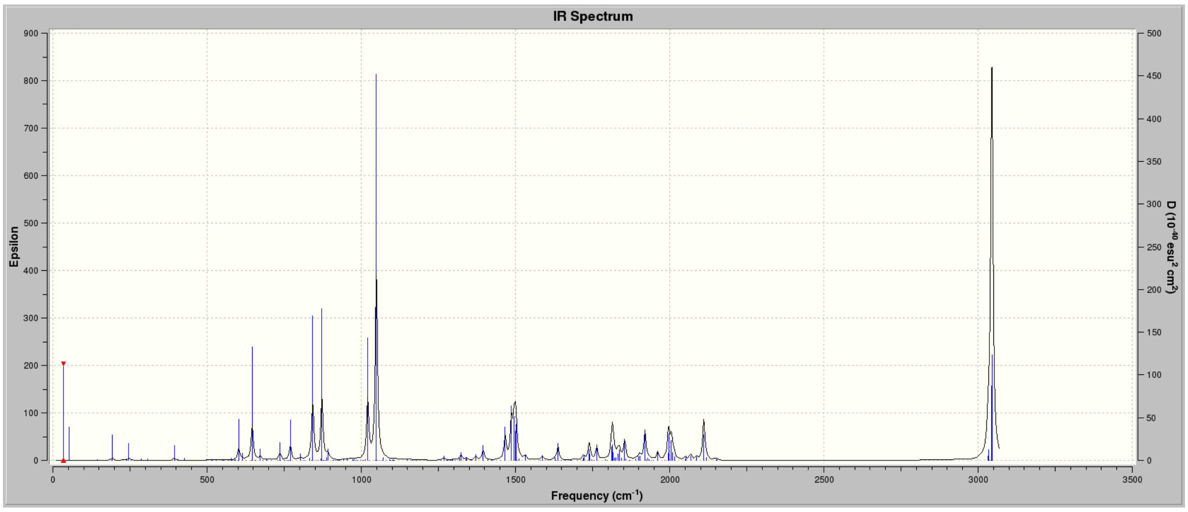

Figure 11: $C_{66}H_{20}$ spectrum, using the MM method.

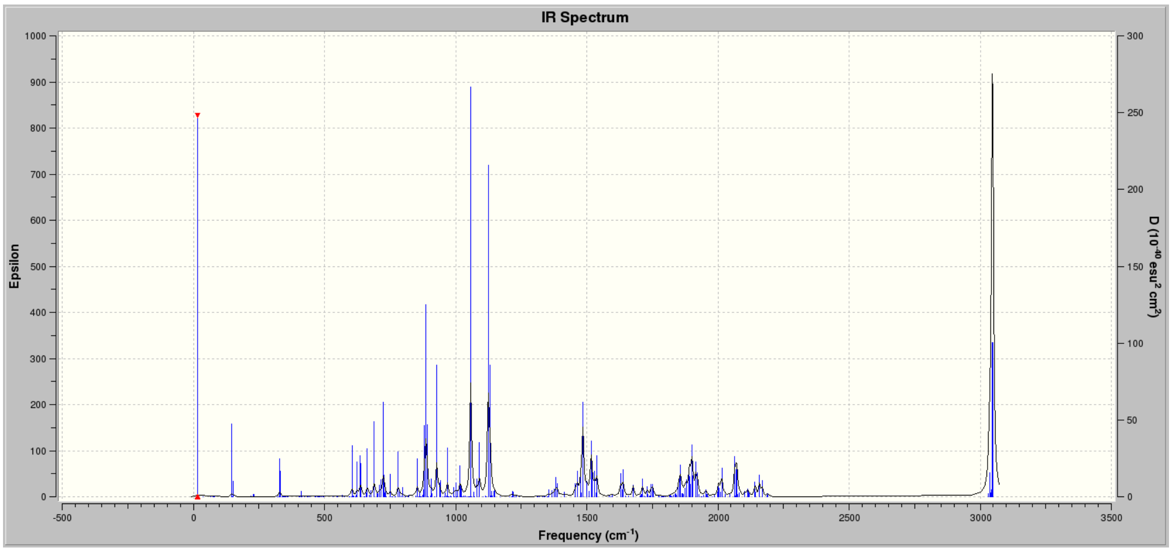

Figure 12: Circumcircumcoronene spectrum, using the MM method.

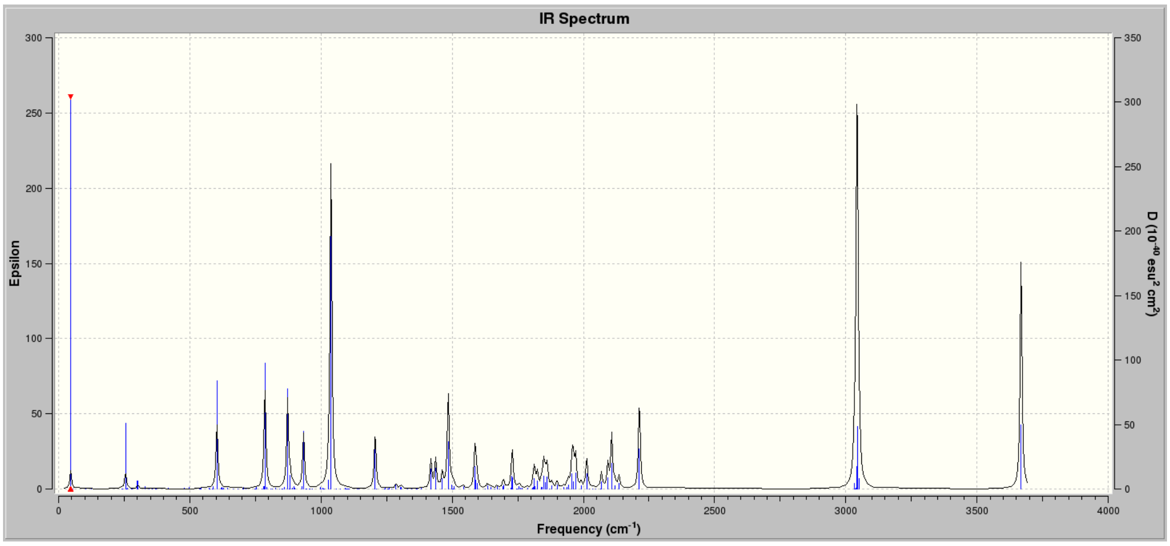

Figure 13: $C_{53}H_{18}N^{+}$ spectrum.

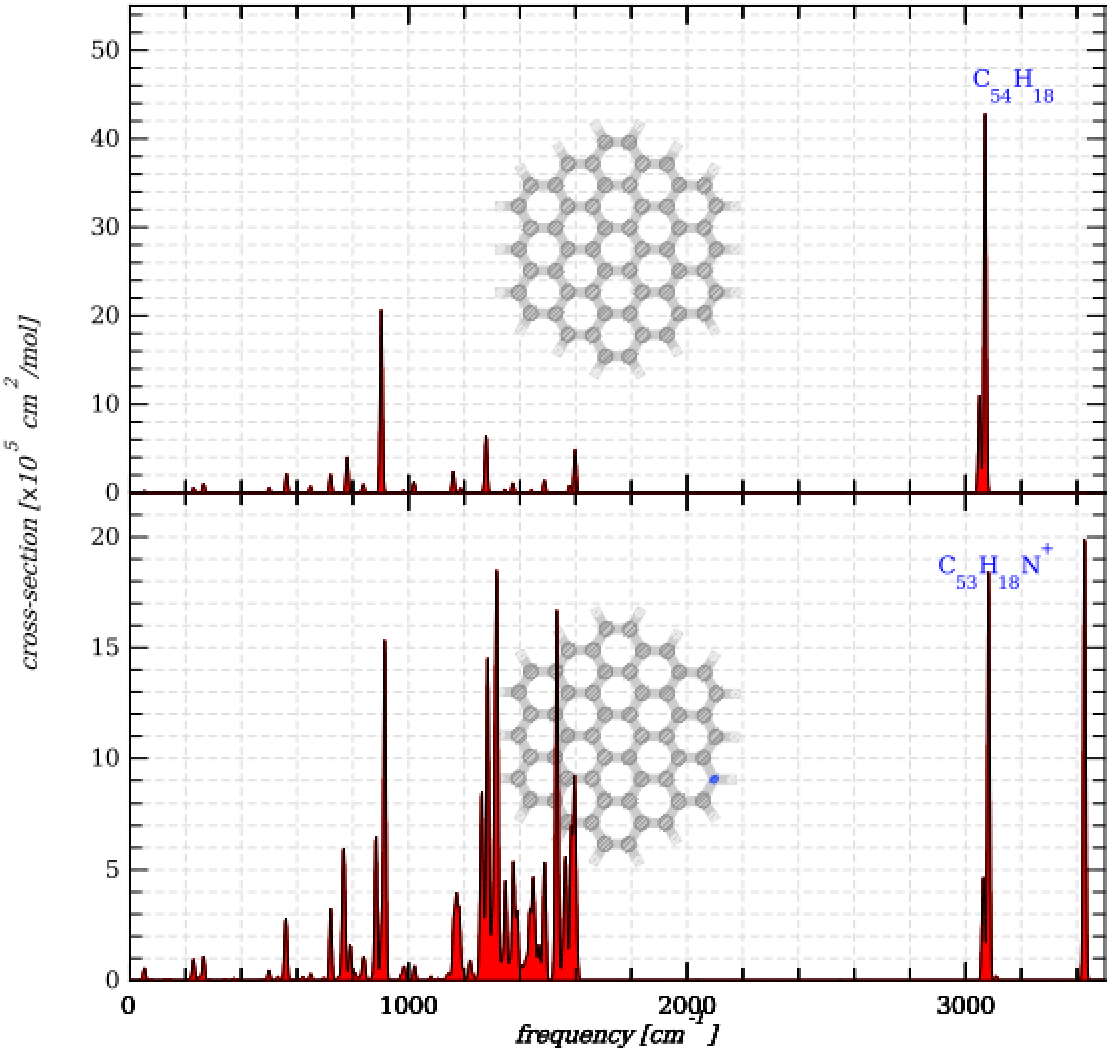

Figure 14: Comparison of $C_{54}H_{18}$ and $C_{53}H_{18}N^{+}$ spectra.

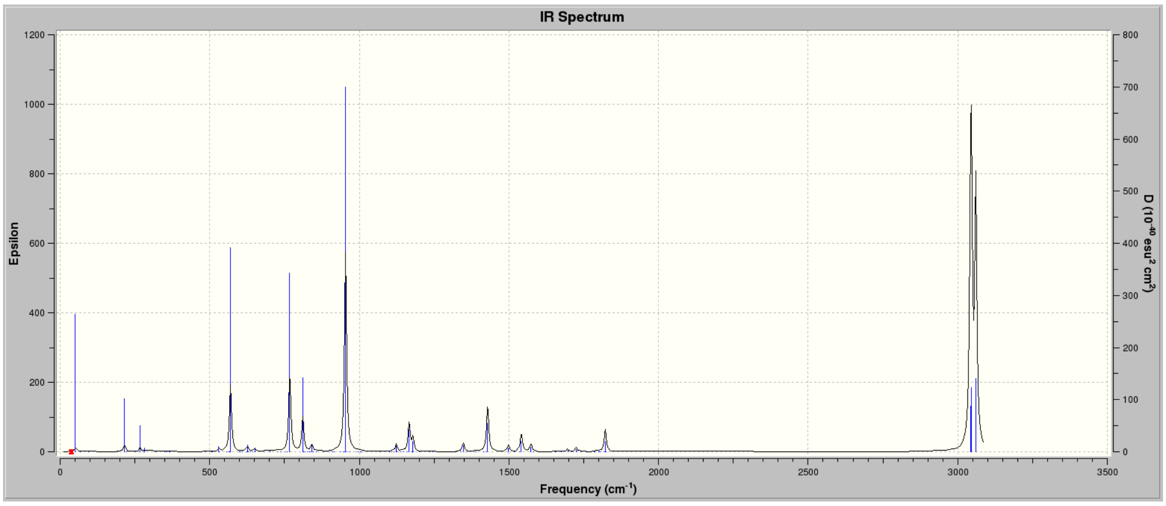

Figure 15: $C_{54}H_{18}$ spectrum calculated using semi-empirical/PM3MM methods.

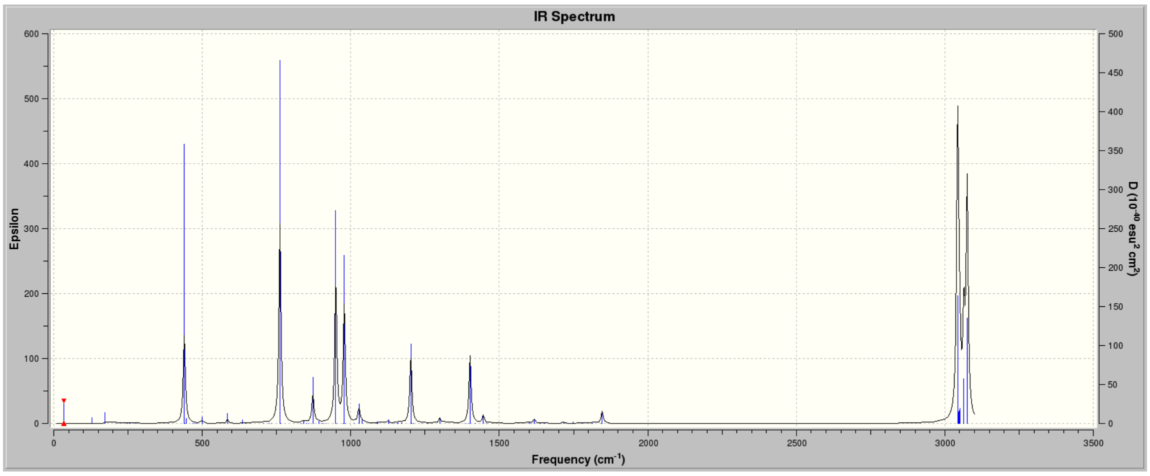

Figure 16: Neutral pentacene spectrum calculated using semi-empirical/PM3MM methods.

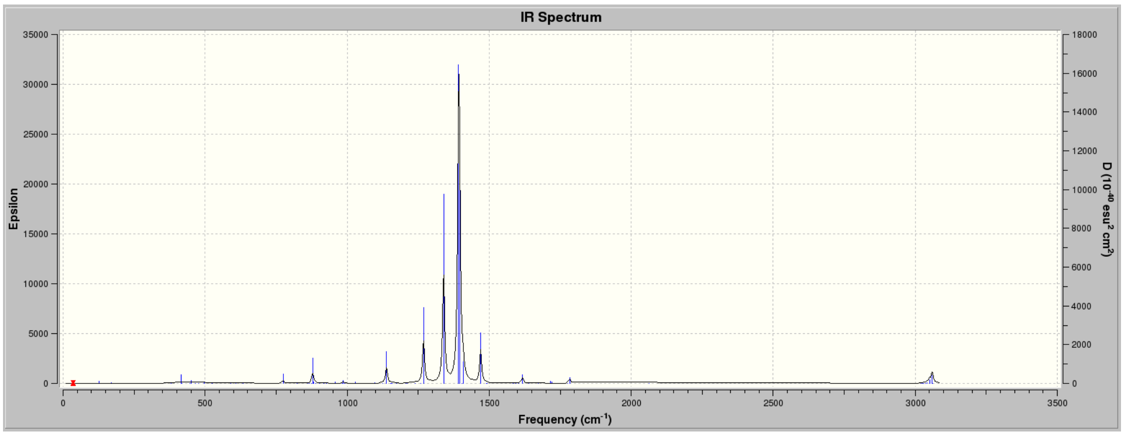

Figure 17: Cationic pentacene spectrum calculated using semi-empirical/PM3MM methods.

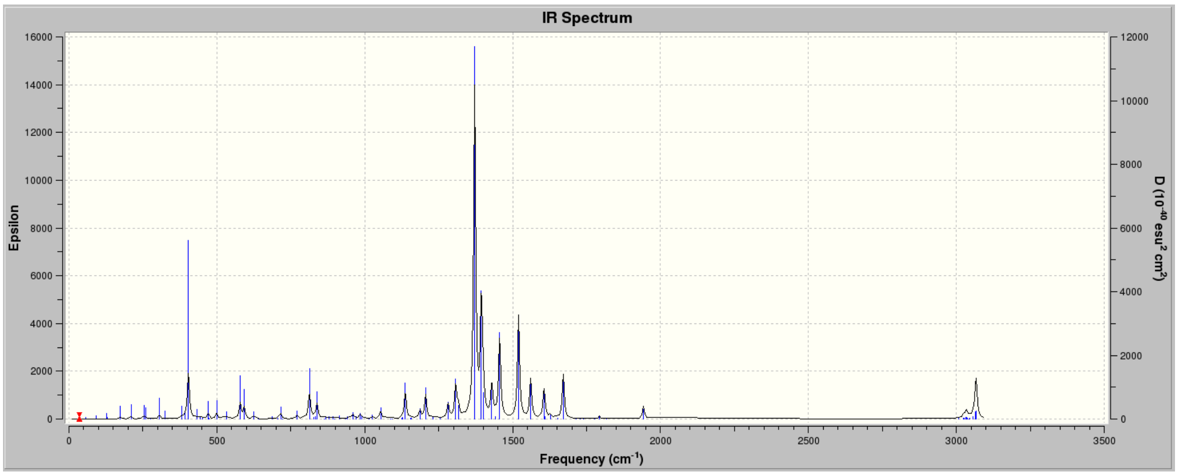

Figure 18: Dehydrogenated cationic pentacene spectrum calculated using semi-empirical/PM3MM methods.

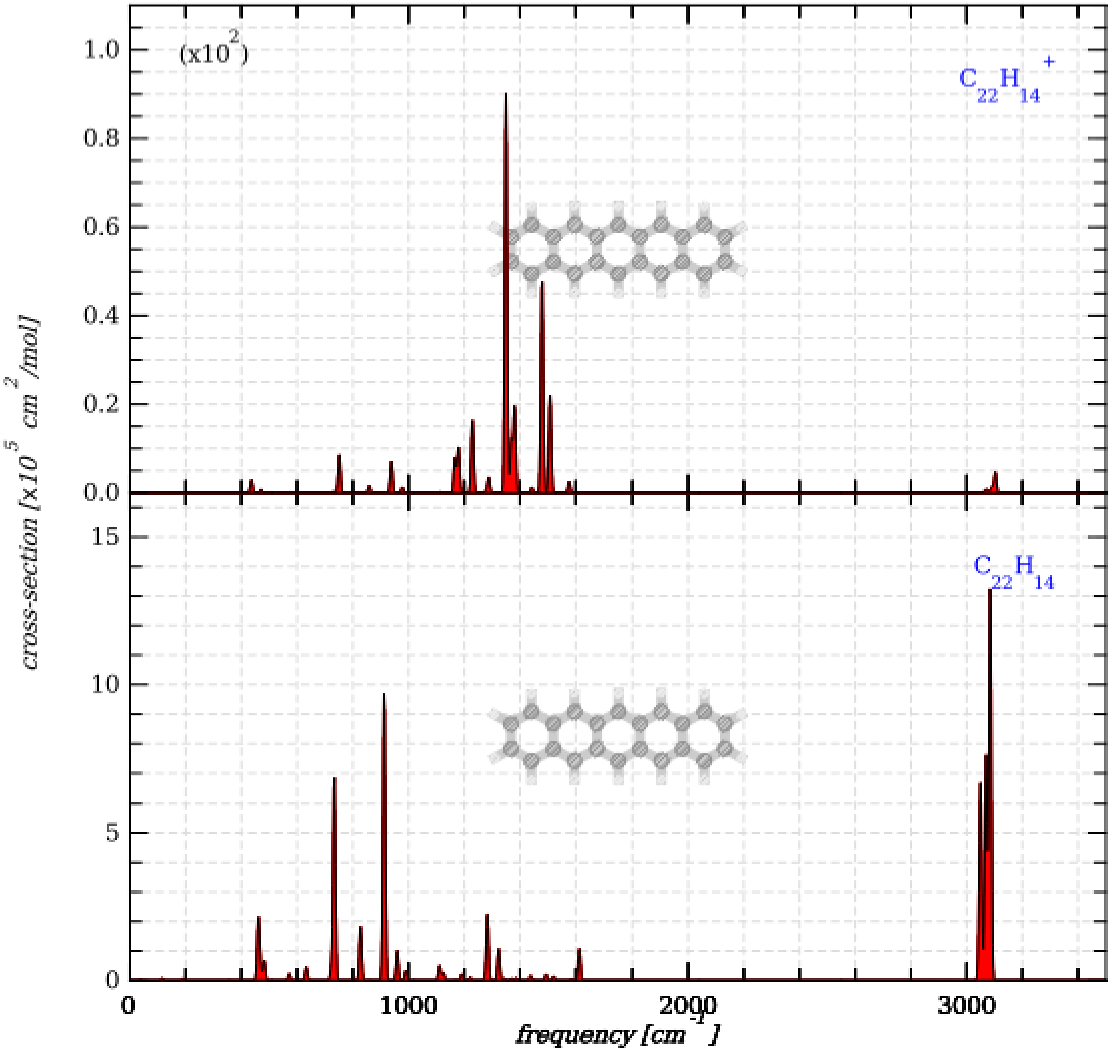

Figure 19: Comparison of neutral and cationic spectra of pentacene obtained from the PAH spectral database.

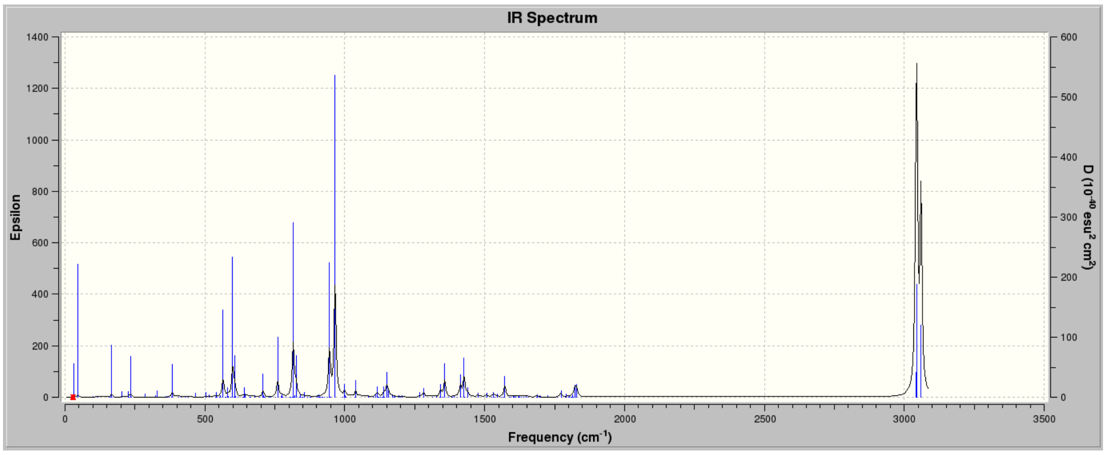

Figure 20: $C_{66}H_{20}$ spectrum calculated using semi-empirical/PM3MM methods.

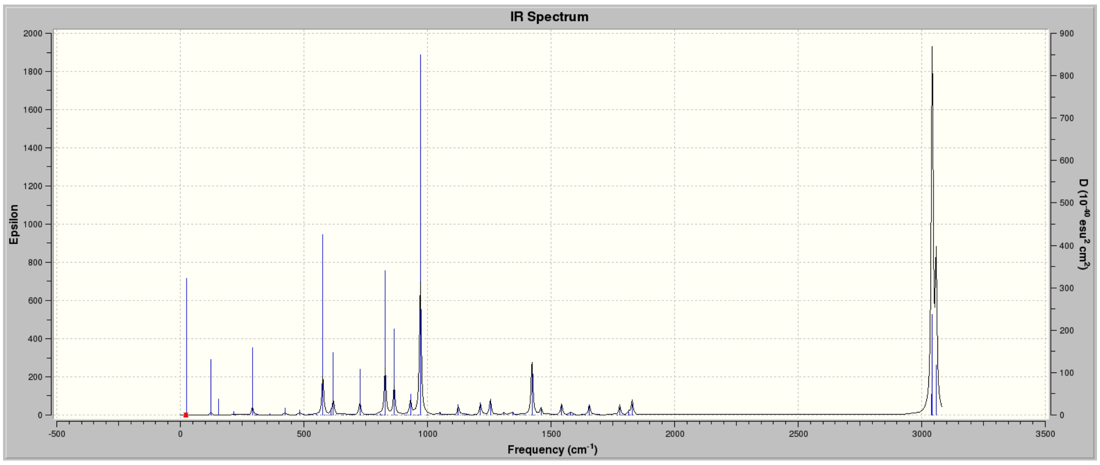

Figure 21: $C_{96}H_{24}$ spectrum calculated using semi-empirical/PM3MM methods.

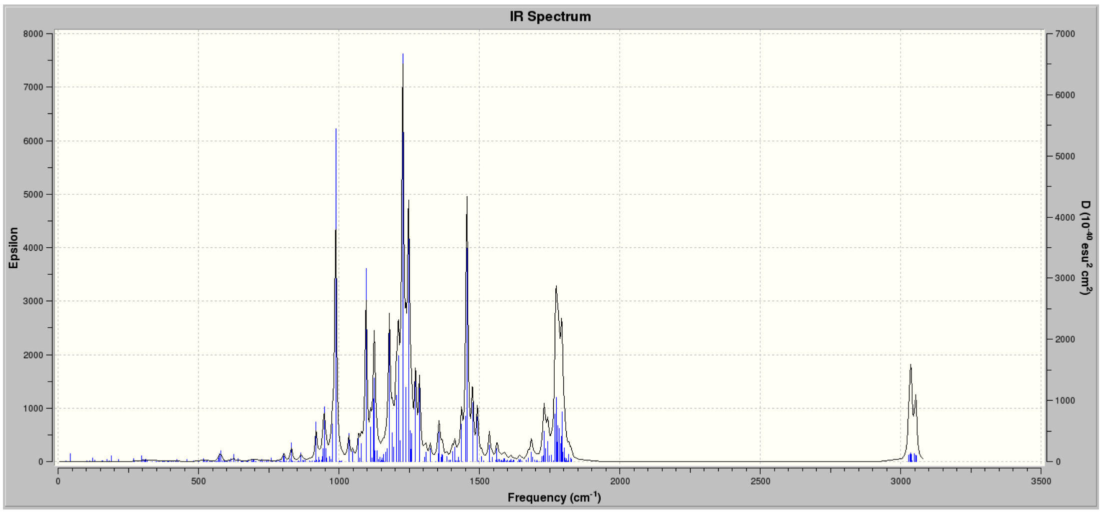

Figure 22: $C_{96}H_{23}^{+}$ spectrum calculated using semi-empirical/PM3MM methods.

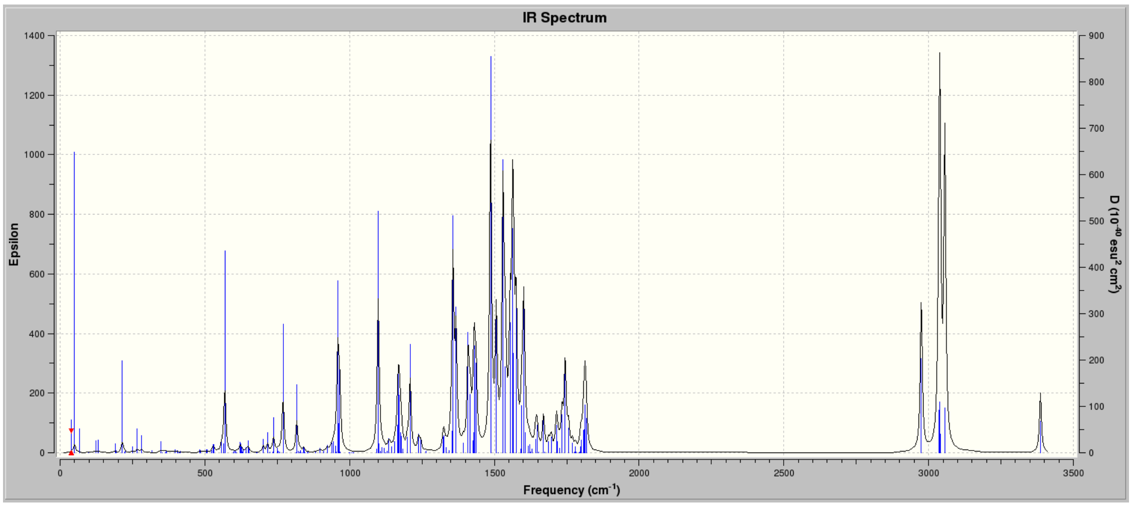

Figure 23: $C_{53}H_{18}N^{+}$ PANH spectrum calculated using semi-empirical/PM3MM methods.

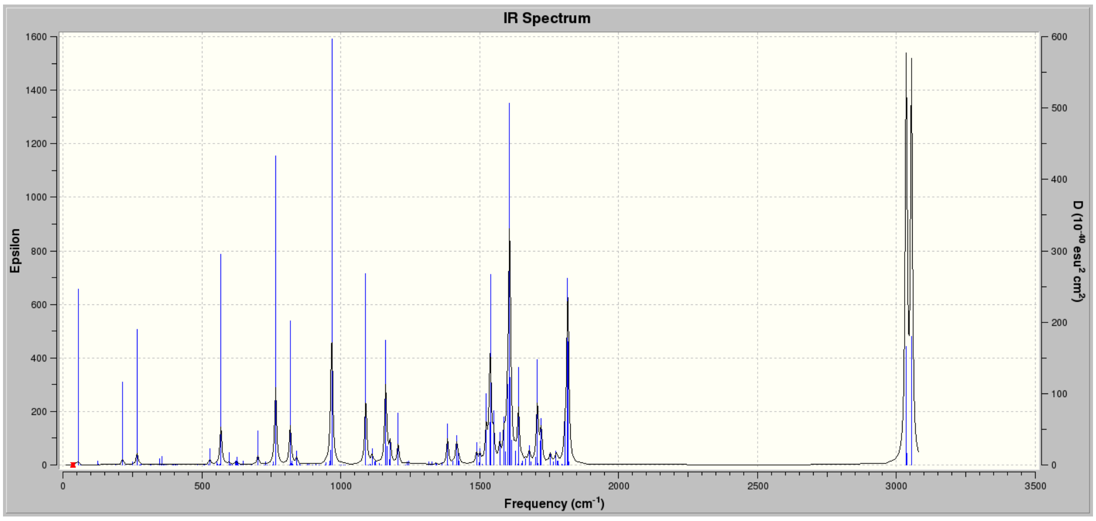

Figure 24: $C_{53}H_{18}N^{+}$ (endoskeletal) PANH spectrum calculated using semi-empirical/PM3MM methods.

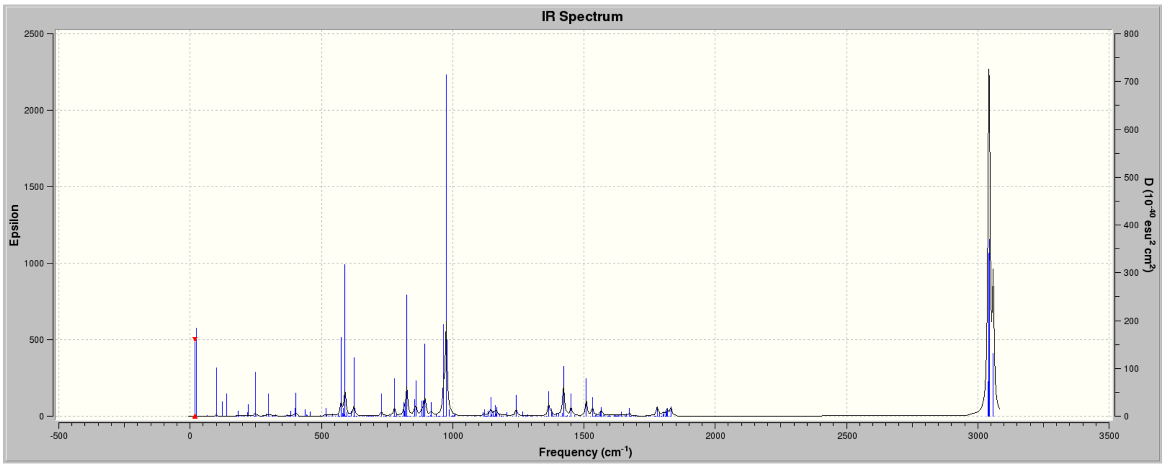

Figure 25: $C_{112}H_{26}$ spectrum calculated using semi-empirical/PM3MM methods.

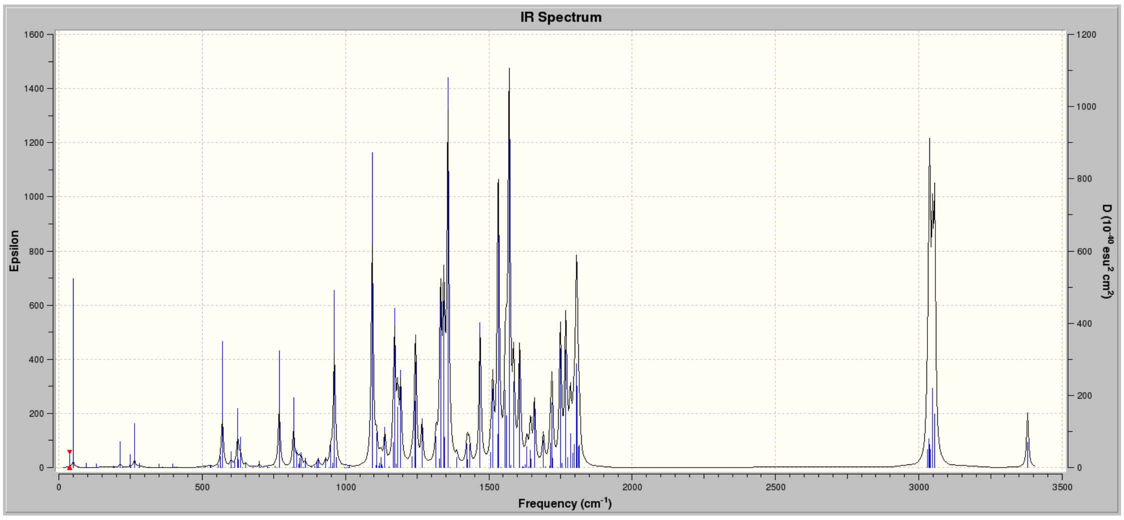

Figure 26: $C_{53}H_{18}N^+$ spectrum, N at (1’), calculated using semi-empirical/PM3MM methods.

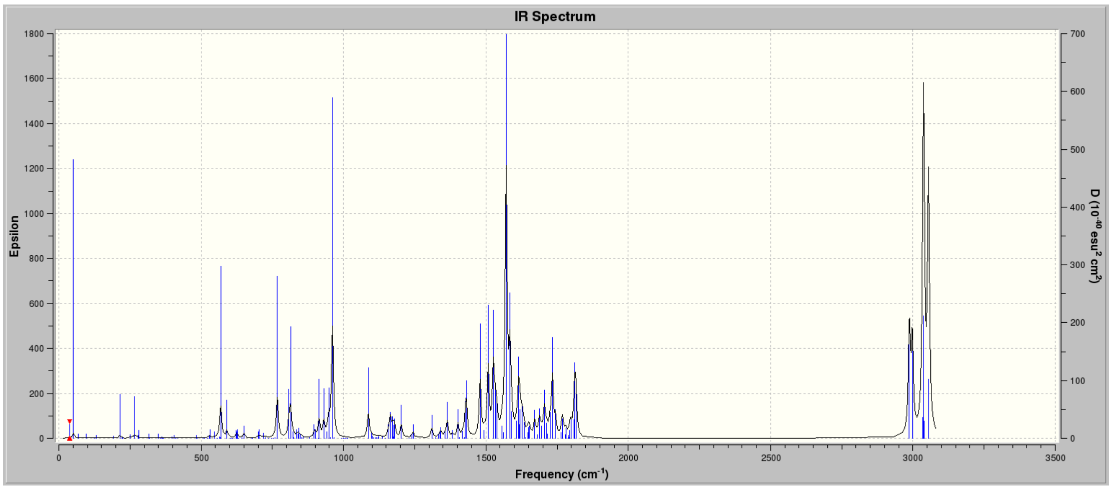

Figure 27: $C_{53}H_{18}N^+$ spectrum, N at (2), calculated using semi-empirical/PM3MM methods.

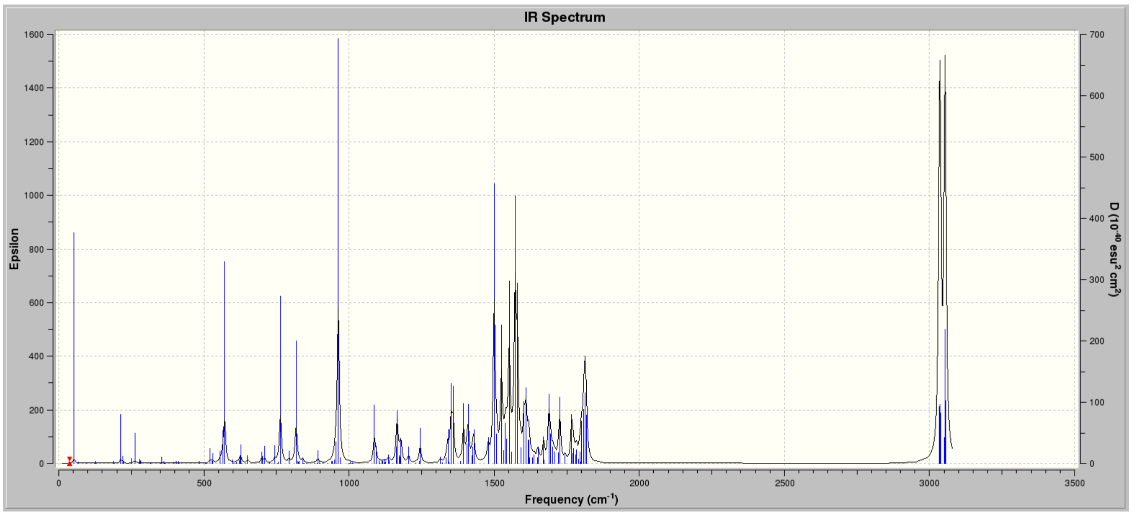

Figure 28: $C_{53}H_{18}N^+$ spectrum, N at (3), calculated using semi-empirical/PM3MM methods.

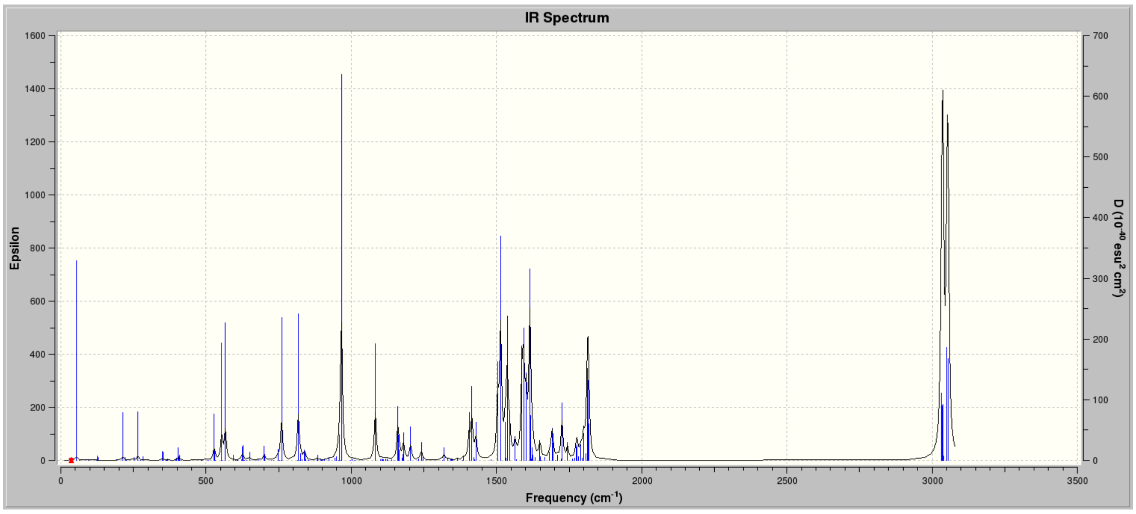

Figure 29: $C_{53}H_{18}N^+$ spectrum, N at (4), calculated using semi-empirical/PM3MM methods.

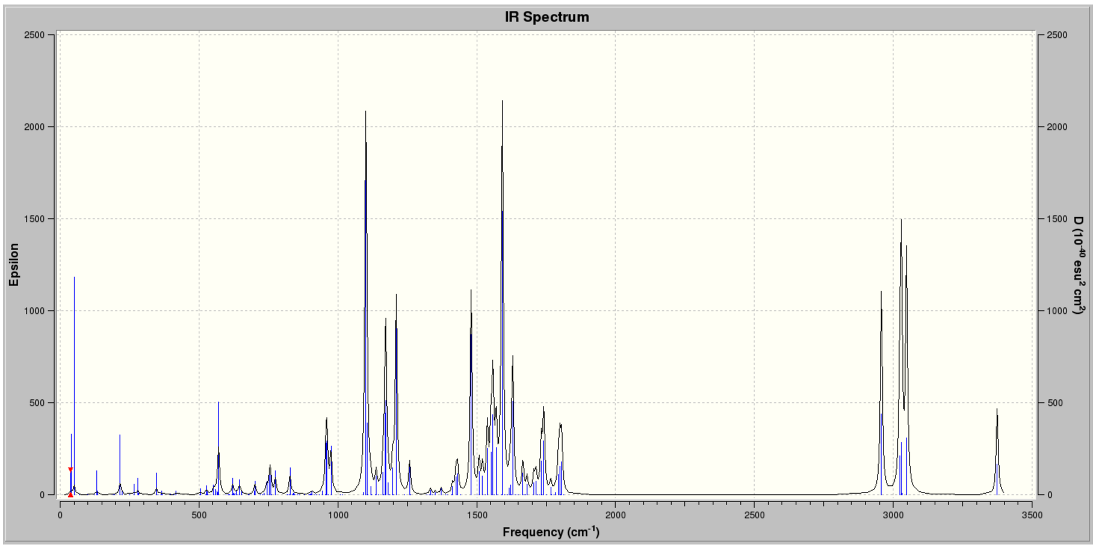

Figure 30: $C_{52}H_{18}N_2^{++}$ spectrum, N's at (1), calculated using semi-empirical/PM3MM methods.

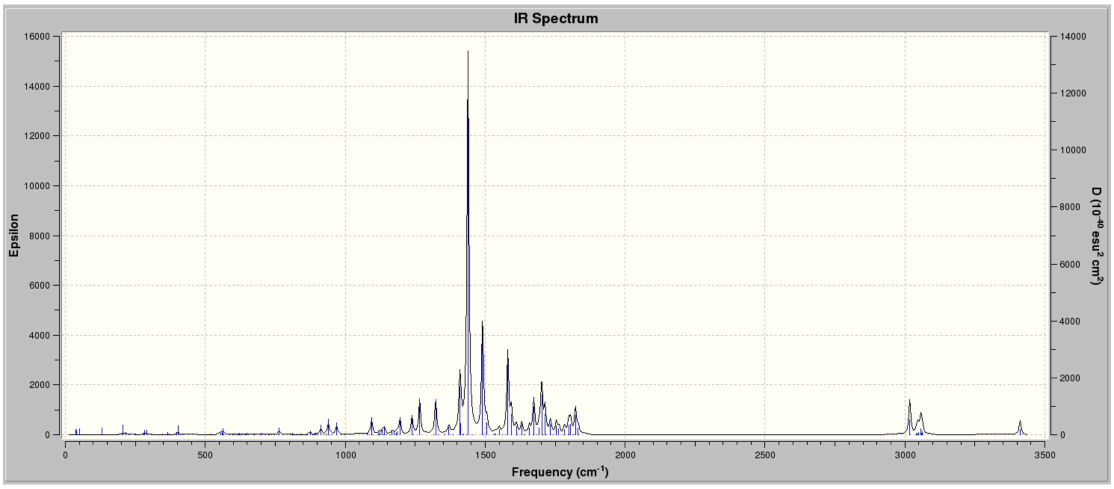

Figure 31: $C_{52}H_{18}N_2^0$ spectrum, N's at (1), calculated using semi-empirical/PM3MM methods.

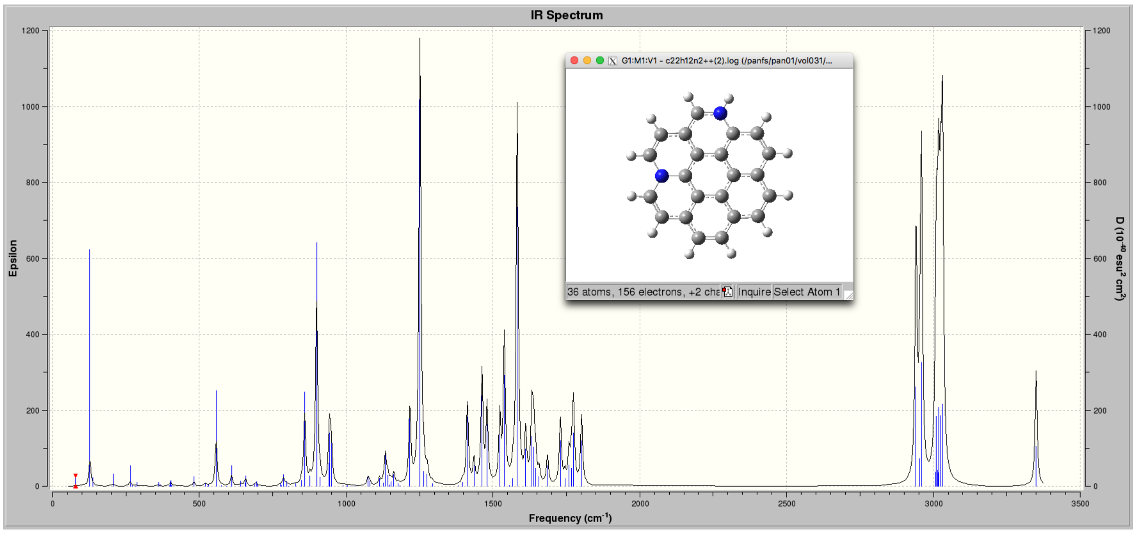

Figure 32: $C_{22}H_{12}N_2^{++}$ spectrum, calculated using semi-empirical/PM3MM methods.

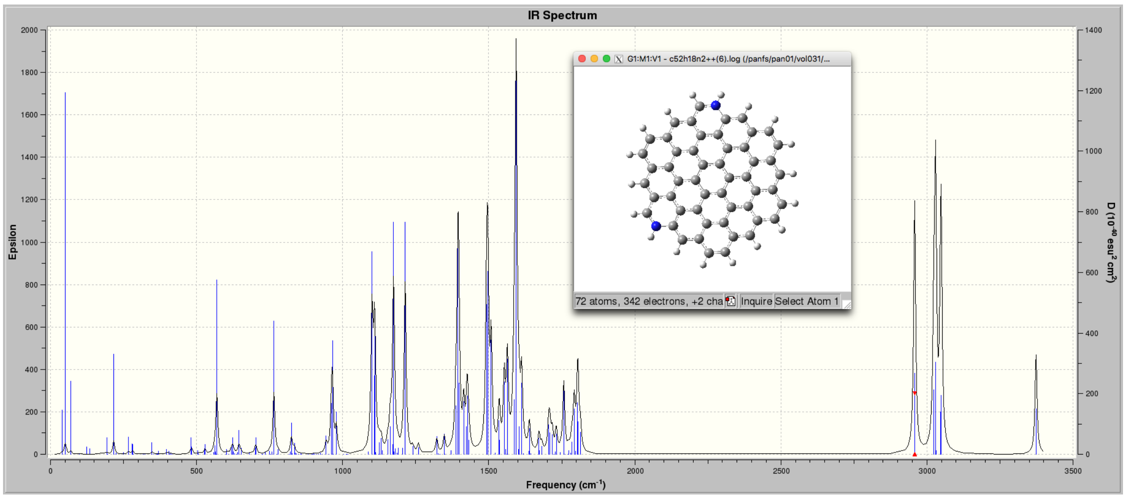

Figure 33: $C_{52}H_{18}N_2^{++}$ spectrum, calculated using semi-empirical/PM3MM methods.

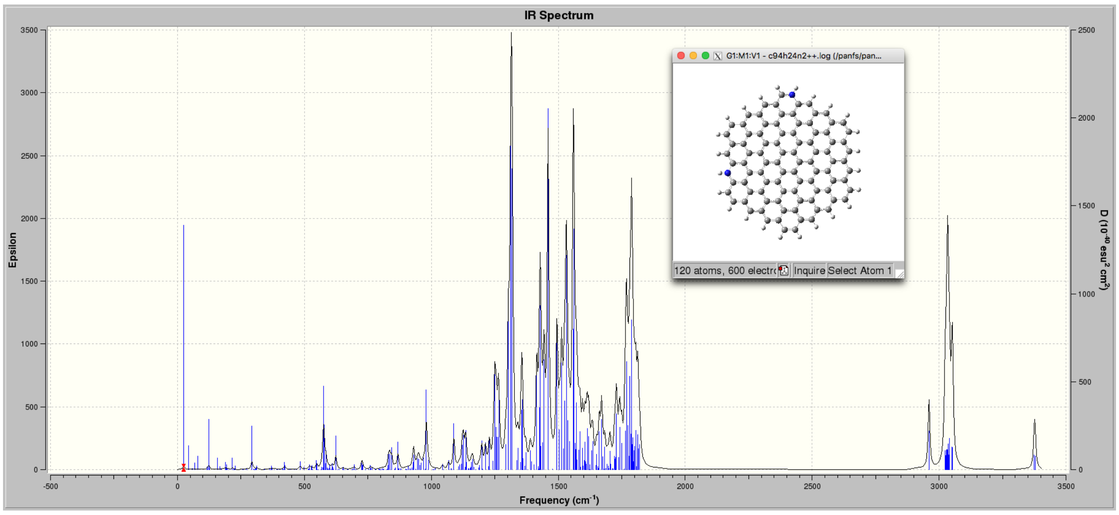

Figure 34: $C_{94}H_{24}N_2^{++}$ spectrum, calculated using semi-empirical/PM3MM methods.

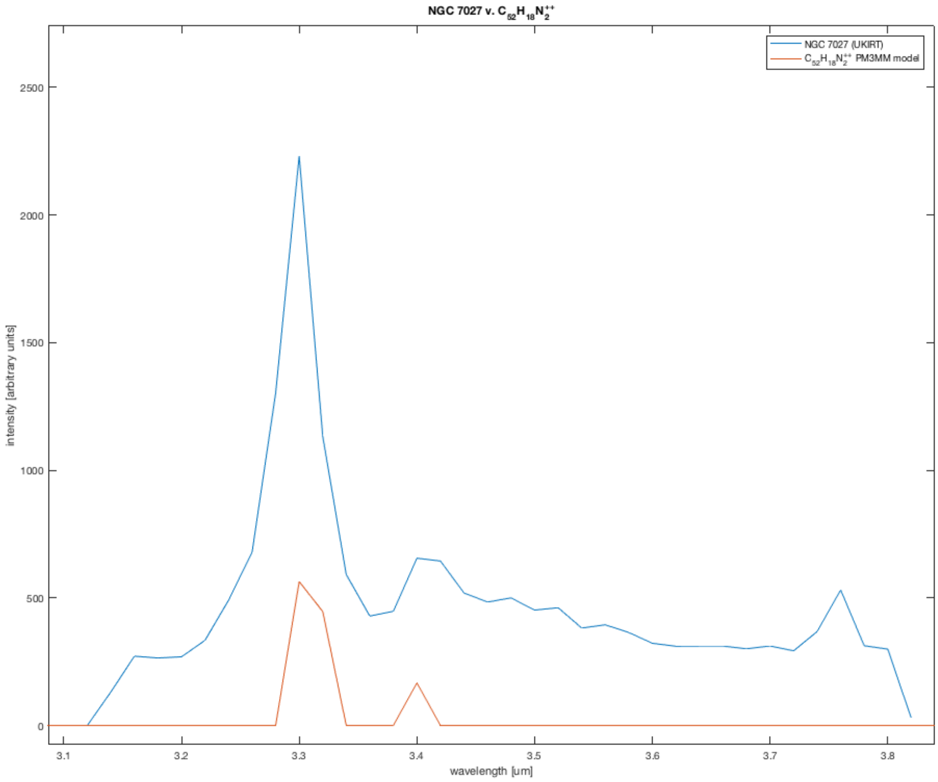

Figure 35: The experimental spectrum of NGC 7027 (blue line) and the calculated (PM3MM) spectrum of $C_{52}H_{18}N_2^{++}$ (red line). The intensities are in arbitrary units and each one has been scaled so that the comparison is easier.

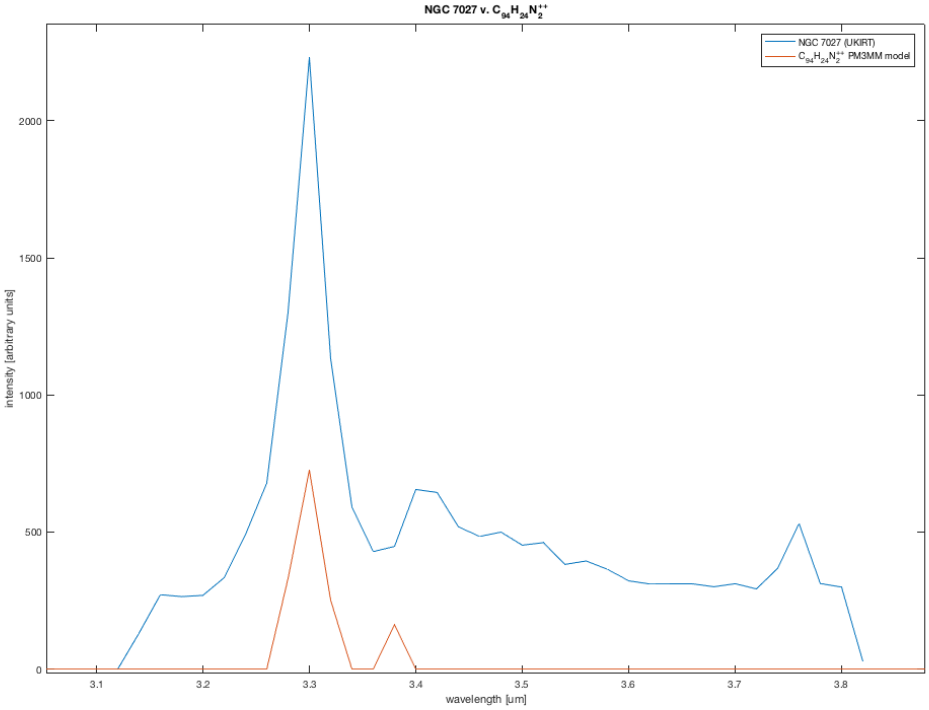

Figure 36: The experimental spectrum of NGC 7027 (blue line) and the calculated (PM3MM) spectrum of $C_{94}H_{24}N_2^{++}$ (red line). The intensities are in arbitrary units and each one has been scaled so that the comparison is easier.

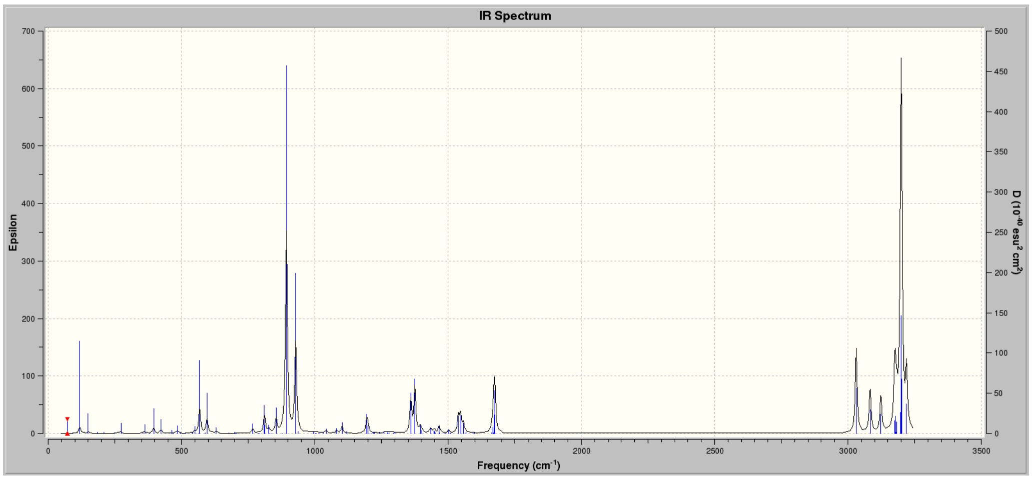

Figure 37: 1-Methylcoronene spectrum, calculated using DFT.

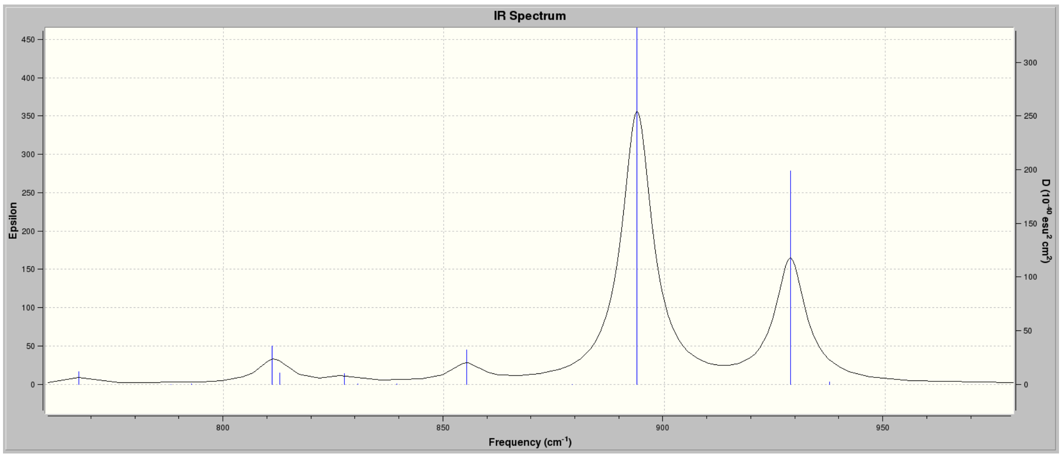

Figure 38: 1-Methylcoronene spectrum (zoomed-in), calculated using DFT.

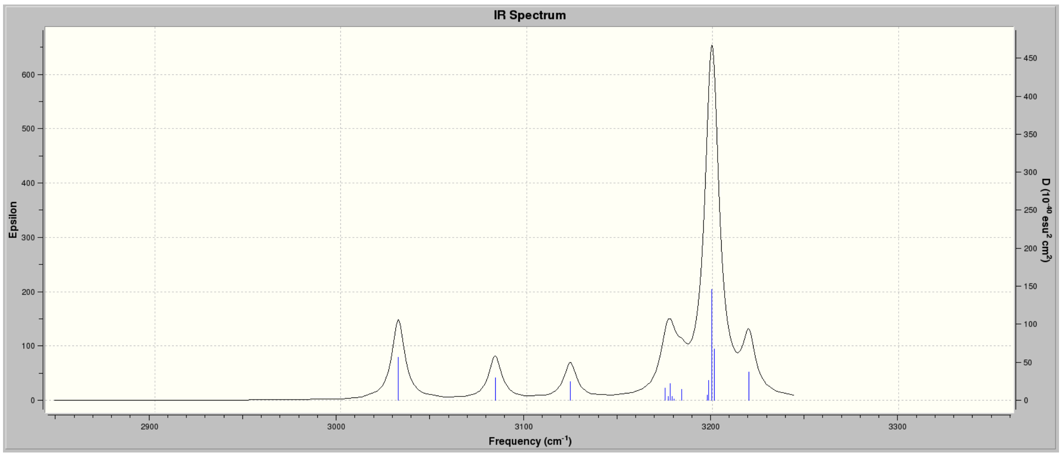

Figure 39: 1-Methylcoronene spectrum (zoomed-in), calculated using DFT.

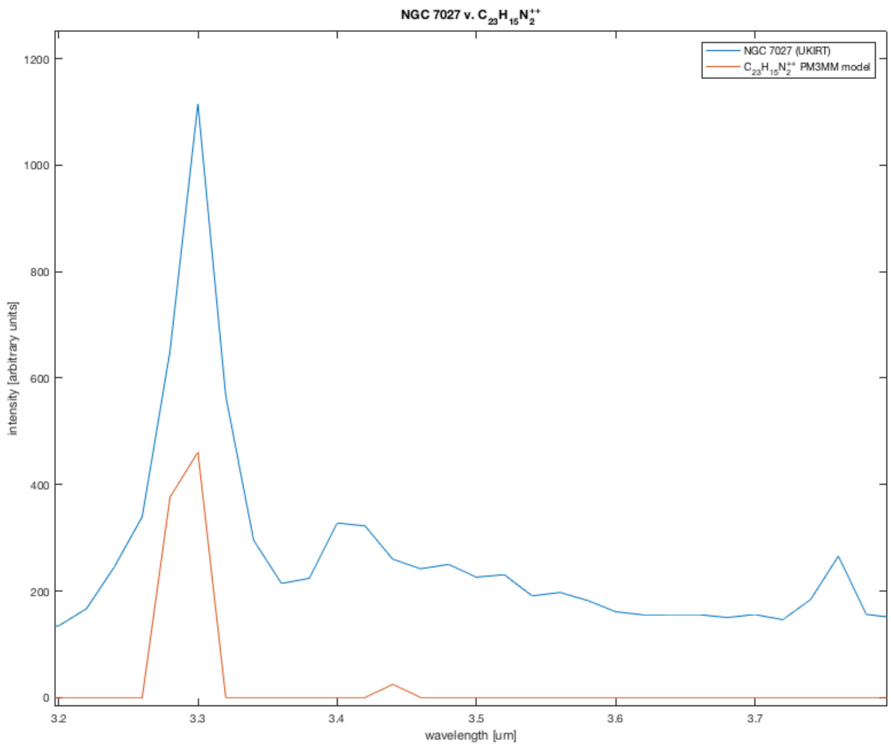

Figure 40: NGC7027 v. $C_{23}H_{15}N_2^{++}$

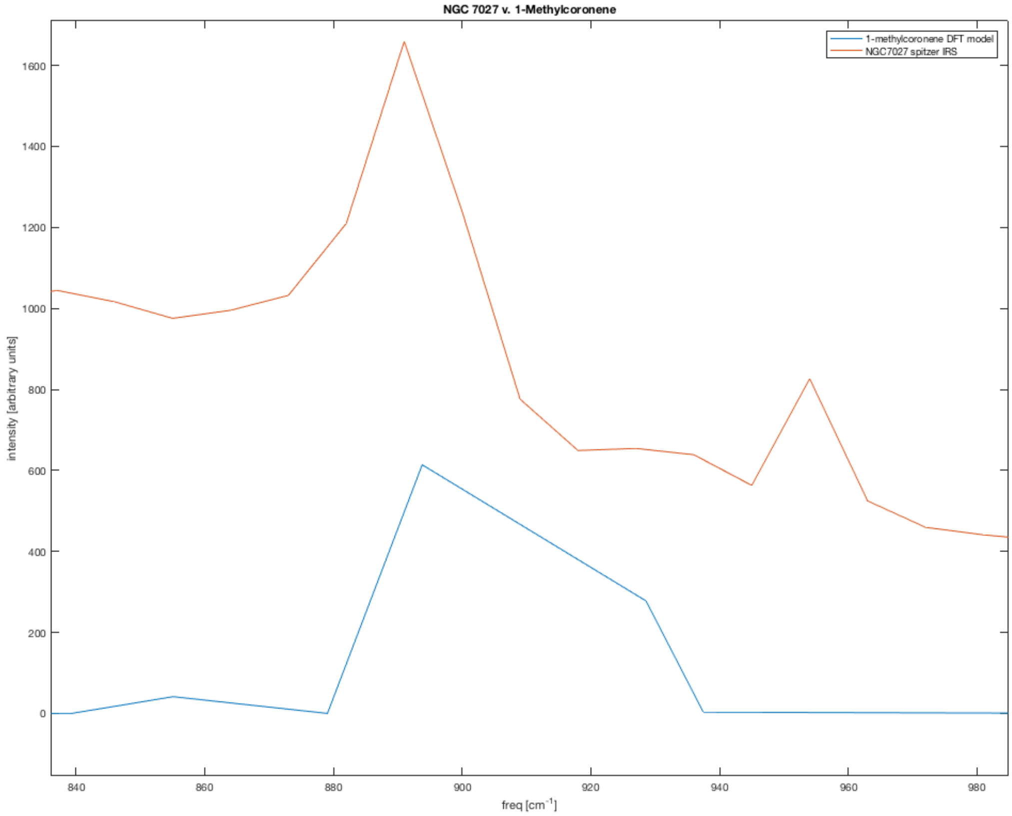

Figure 41: NGC7027 v. 1-Methylcoronene

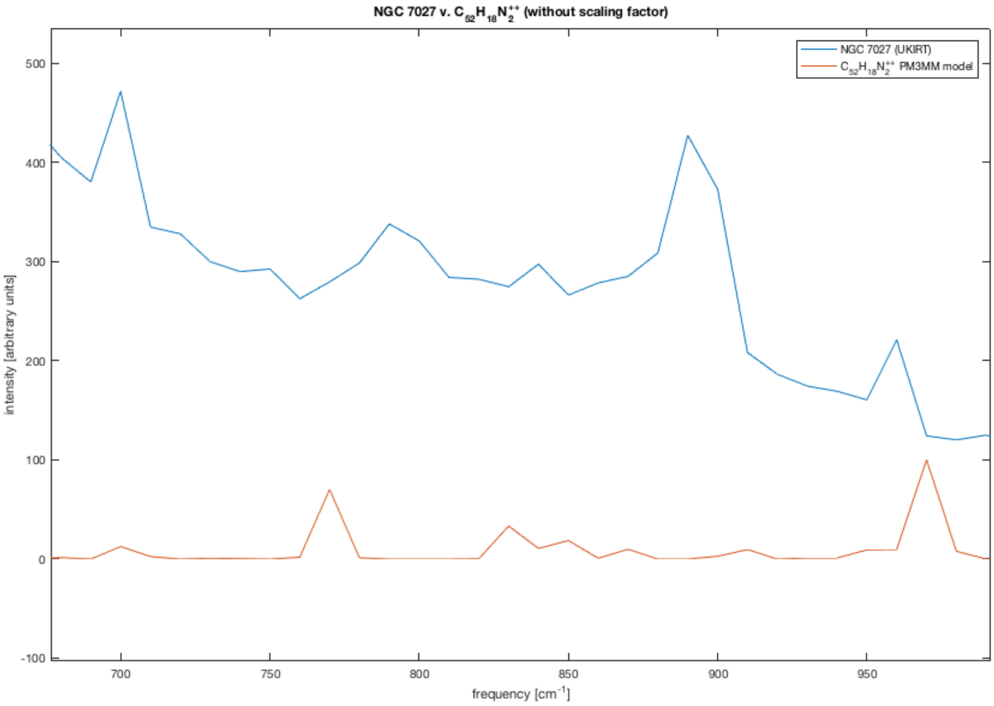

Figure 42: NGC 7027 v. $C_{52}H_{18}N_2^{++}$ (without scaling factor)

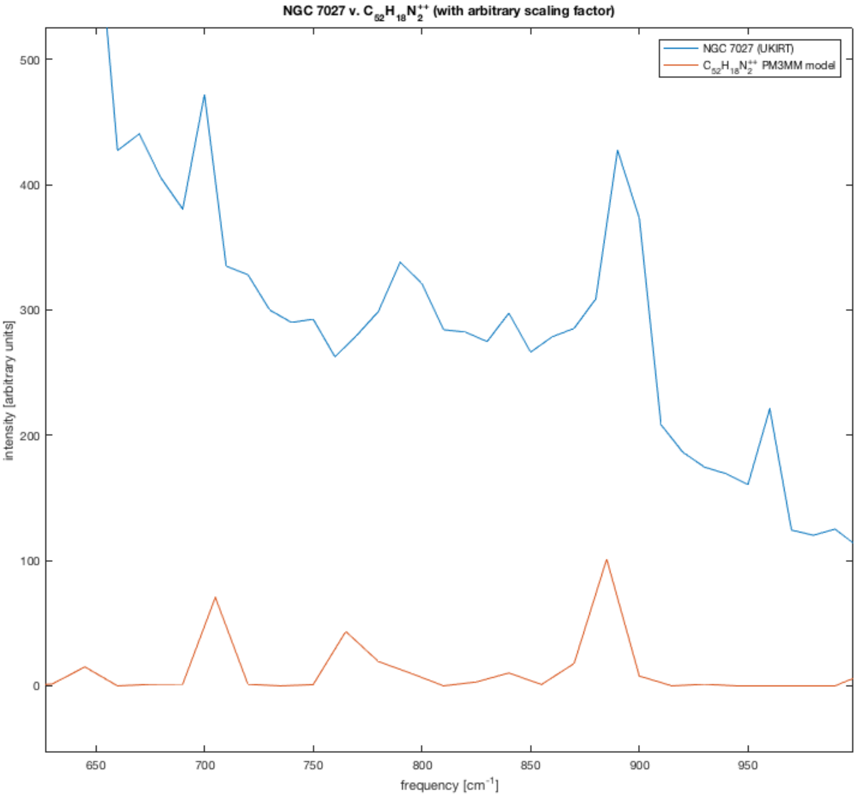

Figure 43: NGC 7027 v. $C_{52}H_{18}N_2^{++}$ (with arbitrary scaling factor)

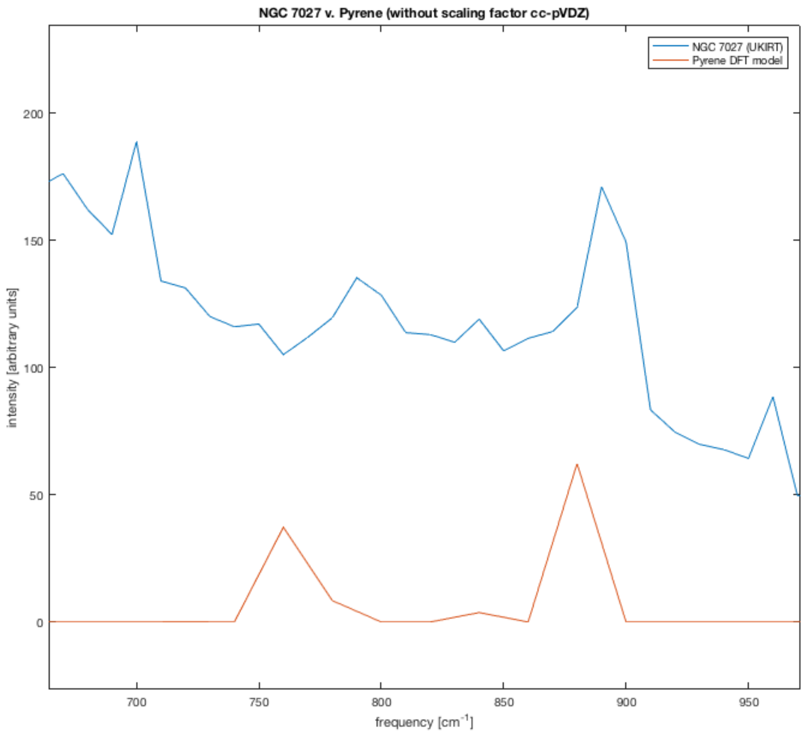

Figure 44: NGC 7027 v. Pyrene (without scaling factor cc-pVDZ)

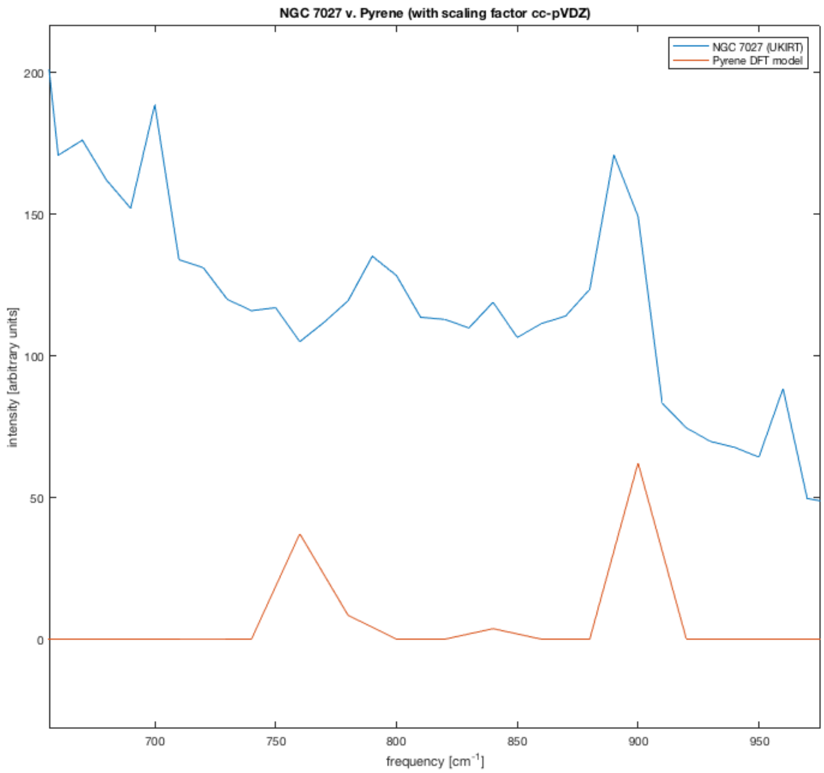

Figure 45: NGC 7027 v. Pyrene (with scaling factor cc-pVDZ)

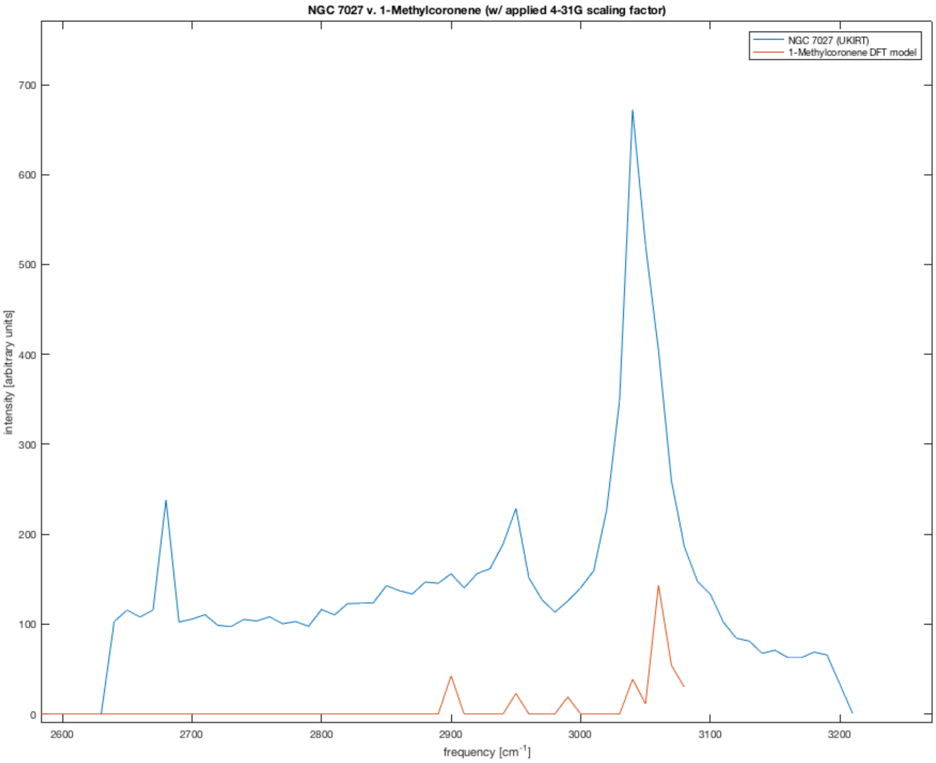

Figure 46: NGC 7027 v. 1-Methylcoronene (w/ applied 4-31G scaling factor)